Kinks in the Frenkel-Kontorova model with long-range interparticle interactions

O. M. Braun, Yu. S. Kivshar,* and I. I. Zelenskaya
Institute of Physics, UkrSSR Academy of Sciences, 46 Science Avenue, Kiev 252028, U.S.S.R.
(Received 12 June 1989)

We study a nonlocal Frenkel-Kontorova model that describes a one-dimensional chain of atoms moving in a periodic external potential and repulsing one another according to a long-range law, e.g., the power law $\sim x^{-n}$. The investigation is carried out both numerically and analytically in approximations of a weak or strong bond between atoms. Static characteristics of kinks (topological solitons) such as the effective mass, shape, and amplitude of the Peierls potential, the interaction energy of kinks, and the creation energy of kink-antikink pairs are calculated for different (exponential and power with $n=1$ and 3) laws of the interparticle interaction and various concentrations of atoms, i.e., ratio between the external potential period and the average spacing of atoms in the chain. The anharmonicity of the interaction potential between atoms is shown to result in differences between kink and antikink parameters, which are proportional to the value of the anharmonicity that rises with increasing exponent n of the interaction potential as well as at a changeover from a complex to a simpler unit cell. It is noted that at a power law of the interparticle repulsion this law describes also the asymptotics of the kink shape as well as the interaction energy of the kinks. Because of this, the dependence of, e.g., the amplitude of the Peierls potential versus the atom concentration, is similar to the "devil's staircase." The applicability of the extended Frenkel-Kontorova model for describing diffusion characteristics of a quasi-one-dimensional layer adsorbed on a crystal surface is discussed.

I. INTRODUCTION

The study of nonlinear phenomena in layers adsorbed on crystal surfaces is of a great interest from both fundamental and applied viewpoints.[1,2] In some cases adsorbed layers may be treated as quasi-one-dimensional systems. For example, at adsorption of atoms on steplike (vicinal) surfaces of semiconductors[3] atoms are predominantly adsorbed along steps where they have a higher bond energy since surface atoms of the semiconductor substrate have excessive ("broken") bonds on the step. A second example refers to adsorption on "furrowed" metal faces[1] [such as the (112) face of a bcc crystal], where the substrate potential in one direction is much less than in a direction perpendicular to it so that adsorbed atoms (adatoms) situated in one "furrow" can be approximately regarded as a quasiindependent chain of adatoms.

For studying the nonlinear dynamics of atoms in the one-dimensional systems the Frenkel-Kontorova (FK) model, which describes the behavior of a harmonic atomic chain in a periodic external potential, has been successfully used (see, e.g., Ref. 4); for the system of adatoms the periodic potential is the substrate potential. In the long-wave limit, excitations of the Frenkel-Kontorova model are described by a nonlinear differential equation, such as the sine-Gordon (SG) equation (see, e.g., Ref. 5). Note that quite a number of physical objects allowing a model description with the aid of the SG equation are known: dislocations in solids,[6,4] domain walls in magnetic materials (see, e.g., Ref. 7), vortices in long Josephson junctions,[5] charge-density waves in quasi-one-dimensional conductors (see e.g., Ref. 8), etc.

For the SG system, as well as any nonlinear system for which the density of the potential energy has, at least, two equivalent vacuum states (i.e., states corresponding to a minimum of the system energy), there exist solutions (the so-called kinks) which describe transitions between the states. For adsystems, a homogeneous vacuum solution of the SG equation describes a commensurate structure when all adatoms lie in the minima of the substrate potential, while a kink- (antikink-) type solution describes the dynamics of an excessive adatom (adatom vacancy) in the commensurate structure (see, e.g., Ref. 9). The motion of such excessive adatoms along the chain corresponds to the motion of kinks, and, therefore, analyzing the motion of kinks is important in the investigation of the surface diffusion and drift of adatoms.[10]

The exactly integrable SG equation has the following property. Any state of the system can be represented as a set of noninteracting quasiparticles: "phonons" (linear excitations), breathers (dynamical solitons), and kinks (topological solitons) (see, e.g., Ref. 11). Note that mass is transferred only by motion of kinks.

Within the scope of the SG equation, kinks move freely and their collisions are elastic.[5,11] For real physical systems, the account of various disturbances and of a more complex character of atomic interactions breaks the exact integrability of the initial SG equation, leaving the possibility for describing the system dynamics in terms of the same quasiparticles which, however, now interact with one another. This interaction, which is due to the departure from a complete integrability, results in the following effects. (a) The Kolmogorov-Sinai entropy becomes nonzero, and the Fourier spectrum of excited

states of the system becomes continuous (see, e.g., Ref. 12). However, there remain peaks in this spectrum caused by the dynamics of breathers and kinks. (b) Corrections to characteristics of quasi-particles (their shape, effective mass, excitation energy, etc.) appear. (c) Motion of the quasiparticles is accompanied by a loss of their kinetic energy, with the result that a moving kink is slowed down right up to a full stop and the amplitude of breather oscillations decreases right up to its vanishing (see, e.g., Ref. 5). (d) Collisions of the quasiparticles become inelastic. This effect is especially substantial for the collision of a kink and an antikink, since it may result in the formation of their coupled breatherlike state with a subsequent vanishing of the latter (see, e.g., Refs. 13–15).

The following perturbations are most important for adsystems.

(1) *Discreteness of adatomic chain.* In the discrete atomic chain a free motion of a kink corresponding to a continuum SG equation is substituted with its motion in a periodic Peierls potential whose amplitude ε_p is always less than the amplitude of the substrate potential, ε_A. Parameters of a kink moving in the Peierls potential change periodically, which results in radiation of phonons (radiation braking of the kink motion), followed by its pinning. These effects were first described in Ref. 16, and then studied in detail both numerically[17–19] and analytically by the perturbation theory.[20–22]

(2) *Long-range character of adatom interactions.* The standard Frenkel-Kontorova model only takes into account interactions of nearest neighbors; the harmonic approximation,

$$v(x)=\tfrac{1}{2}(l/\pi)^2(x-\bar{a})^2 \tag{1.1}$$

(where $\bar{a}$ is the equilibrium distance between particles and parameter l characterizes the magnitude of interaction between adatoms), is assumed for the pair potential of interaction, $v(x)$.

However, in real adsorption systems interaction between particles is more complicated (see Ref. 23). In particular, if adatoms are charged, then the Coulomb repulsion $v(x)\simeq e^2/x$ (Ref. 24) (e is the adatomic charge) acts between them at distances $x<a^*$ (where a^* is the screening radius, which is equal to the Debye screening radius for a semiconductor substrate and to the inverse Thomas-Fermi momentum for a metallic substrate). For a semiconductor substrate the value of a^* is large enough, and the law $v(x)\sim x^{-1}$ is the main one. For adsorption on a metallic substrate the value of screening radius a^* is of the order of the lattice constant; at distances $x\gtrsim a^*$ the interaction of adatoms has of a dipole-dipole character: $v(x)\simeq 2p_A^2/x^3$,[1,25] p_A being the dipole moment of an adatom. If adatoms are neutral, then the overlap of their electronic shells results in a "direct" interaction, exponentially decreasing with distance: $v(x)\sim\exp(-\beta x)$.[23] More complex interaction laws are possible as well, such as for the so-called "indirect" mechanism of adatom interaction.[23,26]

An exponential interaction between the nearest atoms is described by the potential

$$v(x)=V_0\exp\{-\beta[(x/a_s)-1]\}\ , \tag{1.2}$$

where V_0 is the energy of interaction of atoms occupying nearest adsorption sites; a_s is the period of the substrate potential, and parameter β characterizes the anharmonicity of the potential. In the absence of a substrate potential ($\varepsilon_A=0$), interaction (1.2) results in the well-known equation for the Toda chain[27] where only dynamical solitons can exist. The combination of the Toda-chain equation and the SG equation is a nonintegrable system; static characteristics of such a system were studied in Refs. 28 and 29. The anharmonicity of interaction (1.2) breaks the kink-antikink symmetry of the SG equation;[28] the difference between kink and antikink parameters is determined by the value of the parameter β.

A long-range interaction between adatoms, e.g., of type

$$v(x)=V_0/|x/a_s|^n\ , \tag{1.3}$$

where n is an integer ($n\geq 1$) and V_0 is the energy of repulsion of adatoms occupying adsorption sites ($V_0>0$), leads to nonlocal perturbations in the SG equation. The Frenkel-Kontorova model with interaction (1.3) at $n=1$ was studied numerically in Ref. 30, where height ε_p of the Peierls potential for some particular cases was found. If the substrate potential is high ($\varepsilon_A\to\infty$), then the FK model reduces to a one-dimensional long-range Ising model, first studied in Ref. 31 (see, also, Ref. 32). The ground state of the latter system at temperature $T=0$ is described by the so-called "devil's staircase": for every rational coverage of the substrate with adatoms, $\Theta_0=p/q$ (p and q are integers), there exists a commensurate structure of adatoms; when the coverage Θ increases, the structures replace one another through an infinite sequence of phase transitions[32] (see also Ref. 9).

(3) *Disturbance of sinusoidal shape of substrate periodic potential.* A convenient expression for the substrate potential $v_s(x)$, well describing a real adsystem situation, was suggested in Ref. 13:

$$v_s(x)=\tfrac{1}{2}\varepsilon_A\frac{(1-r)^2[1-\cos(2\pi x/a_s)]}{1+r^2+2r\cos(2\pi x/a_s)}\ , \tag{1.4}$$

where $|r|<1$. At $r=0$ the potential $v_s(x)$ has a sinusoidal shape, at $r>0$, a shape of broad wells separated by narrow barriers, and at $r<0$, a shape of deep narrow wells separated by broad gently sloping barriers (see Fig. 1). the parameter r of this potential is related to frequency ω_0 of oscillations of an isolated adatom at the minimum of the substrate potential:

$$\begin{aligned} &r=(1-\kappa)/(1+\kappa)\ , \\ &\kappa\equiv\omega_0(a_s/2\pi)(2m_A/\varepsilon_A)^{1/2}\ , \end{aligned} \tag{1.5}$$

where m_A is the adatom mass. The potential $v_s(x)$ is produced by the interaction of an adatom with substrate atoms and can, in principle, be calculated from the first principles.[33] However, it is more reliable to determine parameter r directly from experimental data with the help of the equation (1.5) using the measured values of ε_A, the activation energy for diffusion of an isolated adatom,[10] and ω_0, the frequency of adatom oscillations parallel to the surface.[34] Estimates for, e.g., a H/W adsystem

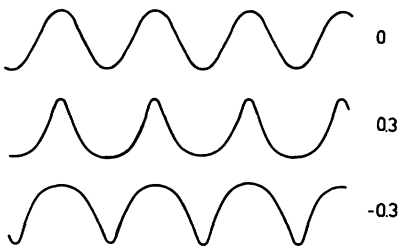

FIG. 1. Substrate potential $v_s(x)$ at different values of the parameter r.

(hydrogen atoms adsorbed on a tungsten surface), yield $r \approx -0.3$.[35]

A departure of a shape of potential $v_s(x)$ from a sinusoidal one results, first of all, in a change of the kink form.[13] The form of a kink is described by shifts of the atoms from the minima of the substrate potential, u_j, j being the number of the atom, or by the function $u(x)$, $x = ja_s$ in the continuum approximation (see Sec. IV). The asymptotics of the function $u(x)$ have the form for a kink with a size d,

$$|u(x)-u(x=\pm\infty)| \simeq (4/\omega_0)\exp[-(|x|/d)\omega_0] , \quad x \to \pm\infty , \tag{1.6}$$

so that $|u| > |u_{SG}|$ for $r > 0$ and $|u| < |u_{SG}|$ for $r < 0$, at $|x| \gg d$. A change in the asymptotics should result in a change in the interaction between kinks (see Sec. VI). The function $u_x(x)$, which is proportional to the density of excess adatoms, becomes more "triangular" (as compared with the solution of the SG equation) for the case of $r > 0$ ($\omega_0 < 1$), and more "rectangular" for the case of $r < 0$ ($\omega_0 > 1$) (see Ref. 13). Secondly, the kink mass also changes:[13]

$$\frac{m}{m_{SG}} = \frac{\omega_0}{(|1-\omega_0^2|)^{1/2}} \times \begin{cases} \tanh^{-1}[(|1-\omega_0^2|)^{1/2}], & r > 0 , \\ \tan^{-1}[(|1-\omega_0^2|)^{1/2}], & r < 0 . \end{cases} \tag{1.7}$$

The m/m_{SG} ratio as a function of the parameter r is shown in Fig. 2. Thirdly, as shown by numerical calculations in Ref. 13, the height of the Peierls potential rises drastically at $r \neq 0$. An approximate dependence $\varepsilon_p(r)$ was derived analytically in Ref. 36, at $r > 0$,

$$\frac{\varepsilon_p}{\varepsilon_{p(SG)}} \sim \exp\left[\pi l \frac{\sqrt{r}(1+\sqrt{r})}{1+r}\right] , \tag{1.8a}$$

and at $r < 0$,

$$\frac{\varepsilon_p}{\varepsilon_{p(SG)}} \sim \cos\left[2\pi l \frac{\sqrt{|r|}}{1+|r|}\right] \exp\left[2\pi l \frac{|r|}{1+|r|}\right] . \tag{1.8b}$$

It is interesting that in the case of $r < 0$, at some values of parameter l, the function $\varepsilon_p(l)$ has local minima. It should also be noted that inelastic effects at collisions of kinks were studied in Refs. 15 and 14.

(4) *Interaction between nearest adatomic chains* which form a quasi-one-dimensional layer of adatoms. The existence of interaction between the chains results in interaction between kinks in neighbor chains; for a weak local interaction this effect was studied in Ref. 37. The interaction of chains completely changes the phase diagram of the adsystem:[9] for a one-dimensional chain at $T \neq 0$ a long-range order in a system is impossible, but at the existence of even a weak interaction between the chains a structure with a long-range order can exist, and a "melting" (an "order-disorder" phase transition) of such a two-dimensional structure will proceed through an intermediate phase with a quasi-long-range order. Note that a "solitonic" diffusion of adatoms in the case of a strong attraction between neighboring chains was dealt with in Refs. 38 and 10.

The present paper aims to investigate the static characteristics of kinks in a one-dimensional discrete chain of atoms interacting according to short-range, i.e., exponential (1.2), or long-range [e.g., power (1.3)] laws and placed into a substrate periodic potential (1.4) at arbitrary concentration Θ_0 of adatoms. In Sec. II of this paper we describe the Frenkel-Kontorova model with a long-range interaction between atoms and give definitions of the quantities characterizing a kink (effective mass, potential energy, and height of the Peierls potential, energy of interaction between kinks, and energy of a kink-antikink pair creation). Section III presents the procedure of numerical calculations and the results of calculating the kink characteristics depending on the magnitude of interaction between adatoms, both for the case of interaction of only the nearest neighbors and for a long-range (Coulomb and dipole) interaction of atoms at different coverages $\Theta_0 = p/q$ with a simple or a complex unit cell. We show that a departure from a standard FK model caused by an anharmonicity of the interaction between adatoms leads to the difference in antikink and kink parameters, the difference between the parameters decreasing both with increasing integers p and q, determining the unit cell, and with decreasing exponent n for a power potential of interaction (1.3). In this section we also report a study of the effect of the form of the substrate periodic relief (1.4) on the kink characteristics. The next section (Sec. IV) presents the explanation of the dependences derived by a numerical calculation and gives analytical expressions for the kink characteristics in the weak cou-

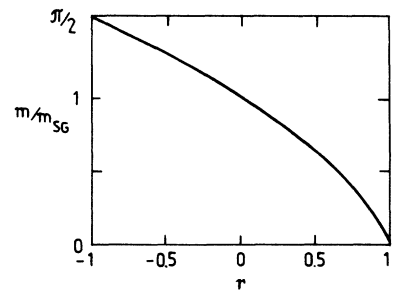

FIG. 2. Effective kink mass as function on parameter r determining the shape of the substrate potential [according to Eq. (1.3) from Ref. 13].

pling limit ($V_0 \ll \varepsilon_A$) and in the long-wave limit ($V_0 \gg \varepsilon_A$) for the case of a short-range potential of adatom interaction. In the case of a long-range adatom interaction, the motion equation in the continuum approximation reduces to an integro-differential equation, which is derived in Sec. V. This equation makes it possible to find the asymptotics of the kink shape at $x \to \pm\infty$ and to determine the law of the kink interaction. This law, which for the power potential of interaction between adatoms is as well a power one, is examined in more detail in Sec. VI. In this section we present also the results of calculation of the dependences of kink parameters on the adatom concentration Θ at a constant value of atom interaction parameter V_0, and show that these dependences at a long-range mechanism of adatom interaction are similar to the "devil's staircase." In Sec. VII we discusses the limitations of the model as well as the possibility of using the Langevin equation to describe the kink motion at a surface diffusion of adsorbates. Finally, the last section (Sec. VIII) presents the conclusions and discusses possible further generalizations of the studied model.

II. MODEL

We will use a Frenkel-Kontorova-type model with a Hamiltonian

$$H = K + V \ , \tag{2.1}$$

$$K = \tfrac{1}{2} m_A \sum_k \left(\frac{dx_k}{dt} \right)^2 , \tag{2.2}$$

$$V = \sum_k \left\{ v_s(x_k) + \tfrac{1}{2} \sum_{k' \geq 1} [v(x_{k+k'} - x_k) + v(x_k - x_{k-k'})] \right\} , \tag{2.3}$$

where x_k is the position of the kth adatom. The quantity K in (2.1) is the kinetic energy of the system, while the quantity V describes the potential energy of adatom interaction with the substrate (1.4), as well as the energy of a pairwise interaction of type of (1.2) or (1.3) of adatoms between themselves. As a vacuum state we take a commensurate structure of adatoms, characterized by coverage $\Theta_0 = p/q$ (p,q are integers) and having a period $a = qa_s$, and a unit cell contains p adatoms so that an average distance between them is $a_A = a/p = a_s/\Theta_0$. Coordinates of adatoms in the commensurate structure can be represented as

$$x_k^{(0)} = x_{(i,j)}^{(0)} = \Delta_i + ja \ , \tag{2.4}$$

where $j = 0, \pm 1, \ldots$ corresponds to the numbers of unit cells, and $i = 1, \ldots, p$, numerates atoms in the cell. The values of Δ_i should be found from the condition of the minimum of vacuum-state energy E_0, determined by the expression

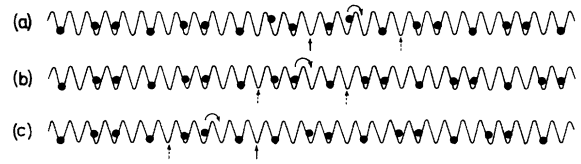

FIG. 3. Structure of the kink (a) and antikink (c) on the background of commensurate structure (b) for the coverage parameter $\Theta_0 = \frac{3}{5}$. A solid arrow shows the kink coordinate before, and a dashed arrow, after displacement of indicated particle to the right.

$$E_0 = \sum_k \left\{ v_s(\Delta_i) + \tfrac{1}{2} \sum_{k' \geq 1} [v(x_{k+k'}^{(0)} - x_k^{(0)}) + v(x_k^{(0)} - x_{k-k'}^{(0)})] \right\} . \tag{2.5}$$

It is obvious that $\Delta_i = 0$ for a simple unit cell ($p = 1$).

We define a kink (antikink) with a topological charge $\sigma = +1$ ($\sigma = -1$) as the minimally possible contraction (extension) of the commensurate structure when in infinity, i.e., for $k \to \pm\infty$, the arrangement of adatoms relative to the minima of the substrate potential coincides with their arrangement in the vacuum state. Owing to boundary conditions, such excitations are topologically stable. For coverage $\Theta_0 = p$ the kink structure is trivial (an excess adatom corresponds to a kink, and a vacancy, to an antikink), but at arbitrary coverage $\Theta_0 = p/q$ with $q \neq 1$ it is more complex. As an example, Fig. 3(a) [3(c)] shows a kink (antikink) on the background of a commensurate structure with coverage $\Theta_0 = \frac{3}{5}$ [Fig. 3(b)]. The arrow in Fig. 3(a) [3(c)] indicates an atom, whose displacement to the right in the nearest minimum of the substrate potential results in a displacement of the kink to the right (antikink, to the left) by structure period a. Similarly, a displacement to the right of the indicated atom in the commensurate structure [Fig. 3(b)] results in the creation of an antikink-kink pair in the system. Note that, as compared with the initial commensurate structure, a kink contains σ/q excess adatoms.

The kink shape is conveniently characterized by quantities

$$u_k = x_k - x_k^{(0)} \ , \tag{2.6}$$

such that

$$\sum_{i=1}^{p} (u_{i,j=+\infty} - u_{i,j=-\infty}) = -\sigma a_s \ . \tag{2.7}$$

Let us consider now an adiabatically slow kink motion. To extract kink coordinate X, we will use the method proposed in Refs. 39 and 21. Quantities $u_{i,j}$ can be represented as $u_{i,j} = f_i(ja - X)$, and therefore, accurate to within an additive constant, we can define the kink coordinate as

$$X = q \sum_k u_k + \text{const.} \tag{2.8}$$

We will select the additive constant so that the point $X = 0$ corresponds to the minimum of the kink potential energy, which is given by

$$E(X)=\sum_k \left\{ v_s(x_k)+\tfrac{1}{2}\sum_{k'\geq 1}[v(x_{k+k'}-x_k)+v(x_k-x_{k-k'})] \right\}-E_0 \ . \tag{2.9}$$

Periodic function $\varepsilon(X)=E(X)-E(0)$ describes the Peierls potential for the kink motion; it has the period a and the amplitude ε_p. In addition, by analogy with expression (1.4) it is convenient to introduce quantity r_p characterizing the shape of the Peierls potential.

When the kink moves along the chain, then $dx_k/dt=(\partial x_k/\partial X)(dX/dt)$, and the system's kinetic energy (2.2) takes the form[21]

$$K=\tfrac{1}{2}m\left[\frac{dX}{dt}\right]^2 , \tag{2.10}$$

where the effective mass of the kink is

$$m\equiv m_A\sum_k(\partial u_k/\partial X)^2 \ . \tag{2.11}$$

Since the kink contains an excess number of adatoms, interaction between kinks at the long-range law (1.3) of interaction between adatoms should as well be of the long-range character:

$$v_{\rm int}^{(0)}(x)=\sigma_1\sigma_2\tilde{V}_0/|x/a|^n \ , \tag{2.12}$$

where x is the distance between kinks. It is obvious that for a simple unit cell ($q=1$), $\tilde{V}_0=V_0$. In the case of a Coulomb interaction of atoms in a chain ($n=1$) the relation between parameters $\tilde{V}_0$ and V_0 can be derived from the following simple consideration (the general case is dealt with in Sec. V). For a commensurate lattice of kinks separated by distance $x=Qa$ the kink interaction energy per a kink is

$$E'_{\rm int}=\tfrac{1}{2}\left[2\sum_{j=1}^{\infty}j^{-1}\right]\tilde{V}_0/Q \ . \tag{2.13}$$

However, the same lattice of kinks can be considered as a system of excess atoms separated by the distance $x'=qx=qQa\equiv q^2Qa_s$. According to (1.3), the energy of interaction of excess atoms per an atom is

$$E''_{\rm int}=\tfrac{1}{2}\left[2\sum_{j=1}^{\infty}j^{-1}\right]V_0/(q^2Q) \ . \tag{2.14}$$

Taking into account that one excess atom corresponds to q kinks, we obtain from the condition $qE'_{\rm int}=E''_{\rm int}$

$$\tilde{V}_0=V_0/q^3 \ . \tag{2.15}$$

Subtracting the trivial interaction energy (2.12), it is convenient to determine the energy of a kink lattice per a kink as

$$E_\sigma(Q)=E(0)-E'_{\rm int} \ , \tag{2.16}$$

where the summation over k in (2.9) and (2.5) should be limited to atoms occupying a length Qa. At $Q\to\infty$ we obtain with the use of (2.16) the energy of creation of a pair of kink-antikink's, separated by an infinite distance, in the initial commensurate structure:

$$\varepsilon_{\rm pair}=\sum_{\sigma=\pm 1}E_\sigma(\infty) \ . \tag{2.17}$$

It will be convenient to use further a system of units where $m_A=1$, $a_s=2\pi$, and $\varepsilon_A=2$. Thus, the proposed model has the following independent parameters: (1) concentration of initial coverage $\Theta_0=p/q$, on whose background the motion of kinks is studied; (2) amplitude V_0 and law [exponential or power (with $n=1$ or 3)] of interaction between adatoms; (3) when studying interaction between kinks, quantity Q, which determines distance x between kinks ($x=2\pi qQ$); and (4) parameter r, which characterizes the shape of the substrate periodic potential.

III. CALCULATION PROCEDURE AND RESULTS

In numerical calculations, instead of the consideration of the motion of an isolated kink in an infinite chain on the background of some commensurate structure of adatoms with coverage Θ_0, it is more convenient to consider a simultaneous motion of an infinite periodic structure of kinks (the so-called knoidal wave). Let the period of the commensurate structure of kinks be $2\pi M$. Then for calculations it is sufficient to place a chain with finite number N of atoms into a periodic substrate potential with M minima and to impose periodic boundary conditions

$$x_{k+N}=x_k \tag{3.1}$$

on the chain ends. The N and M values should be selected so that a chain with the length $2\pi M$ contains one kink on the background of a commensurate structure $\Theta_0=p/q$. To attain this, the N and M values should satisfy the integer equation

$$qN=pM+\sigma \ . \tag{3.2}$$

The obtained commensurate structure of kinks is characterized by the average coverage

$$\Theta=N/M=\Theta_0+\sigma/(Mq) \ , \tag{3.3}$$

and the distance between kinks is equal to $2\pi M$, so that $Q=M/q$. The selection of N in the numerical calculations was governed by a limited computer time and amounted to $N\gtrsim 20$.

Adiabatic characteristics of the described system were calculated with the use of a computer program whose kernel was the solution of the equations of motion, following from Hamiltonian (2.1):

$$\frac{d^2x_k}{dt^2}+v_s'(x_k)+\sum_{k'=1}^{N^*}[v'(x_k-x_{k-k'})-v'(x_{k+k'}-x_k)]+\eta\frac{dx_k}{dt}=0 \ , \tag{3.4}$$

where $k=1,\ldots,N$, and $v'(x)\equiv dv(x)/dx$. Equation (3.4) also incorporates the friction force $F_k=-\eta m_A dx_k/dt$, which acts as a damping of the atom motion. The number of nearest neighbors, N^*, interaction with which should be taken into account, is selected so that the calculation results do not change at a further increase of the N^* value; in fact, for the used calculation parameters, $N^*\sim 2N$. The procedure of compute simulation can be described by the following stages.

(a) As the initial state we take the values

$$x_k^{(\text{init})}=2\pi k/\Theta\ . \tag{3.5}$$

In cases when the initial state (3.5) results in a "sticking" of the system in a metastable state, the condition (3.5) is substituted by $x_k^{(\text{init})}=2\pi k/\Theta+\pi/N$.

(b) The motion equations (3.4) with the initial conditions (3.5) are being solved during some time t_m, needed for the system to "stop" in the ground state, corresponding to the minimum of the potential energy (2.16). The value of t_m is determined so that at $t\geq t_m$ the condition

$$\left[\sum_{k=1}^{N}(\Delta x_k)^2\right]^{1/2}<\varepsilon$$

is fulfilled, where Δx_k is the change of coordinates in some time region Δt ($\Delta t\simeq 10\pi$) and the ε value determines the calculation accuracy (it was selected as $\varepsilon=5\times 10^{-4}$). Note than in the case of $V_0\gg\varepsilon_A$ the calculations must be conducted with a higher accuracy than in the opposite case of $V_0\ll\varepsilon_A$. Naturally, the time t_m depends on the friction coefficient η; the shortest computer calculation time is achieved at $\eta\simeq\omega_0$.

(c) The atom j_{st} is found whose displacement by some distance Δx (on the condition that the remaining $N-1$ atoms adiabatically follow the atom) results in a kink displacement by period a (see Figs. 3 and 4), so that the system state after the displacement of the atom j_{st} is topologically equivalent to the initial state. The configuration shown in Fig. 4(a) generally corresponds to the ground state of the system (see, however, later the results for the case of $r<0$); in this case, $\Delta x=2(\pi-u_{j_{\text{st}}}^{(gr)})$.

(d) The j_{st} atom is displaced by the distance $\frac{1}{2}\Delta x$ in some steps h ($h\simeq\Delta x/20$). Motion equations (3.4) are solved again at every step, but with the difference that the coordinate of the j_{st} atom is now artificially kept unchanged. At every step of displacement of the j_{st} atom the following characteristics were also calculated: the kink coordinate x (2.8), the effective mass m (2.11), and the kink potential energy E_σ (2.9); i.e., the characteristics of the system at a coordinated motion of the entire lattice of kinks as a whole are determined. Note that the summation over k in formulas (2.8), (2.9), and (2.11) is carried out within the range of 1 to N, and in formula (2.5), of 1 to $N_0=M\Theta_0$, so that, e.g., for a simple unit cell ($p=1$),

$$E_0=M\Theta_0\sum_{j=1}^{N^*}v(ja)\ . \tag{3.6}$$

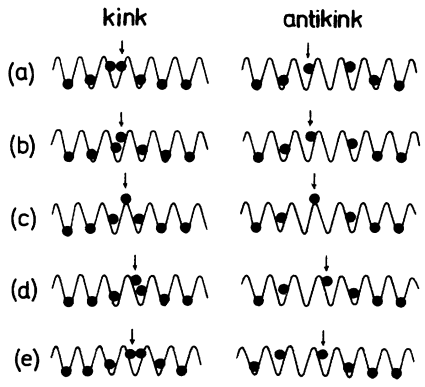

FIG. 4. Adiabatic motion of kink and antikink on the background of the commensurate structure with $\Theta_0=1$. (a)–(e) illustrate successive displacements of a kink at artificial motion of the j_{st} particle (indicated by the arrow). (a) and (e) are initial and final (after kink shift by the period $a=2\pi$) ground states of the system; (c) is the unstable configuration corresponding to the maximum of the kink potential energy.

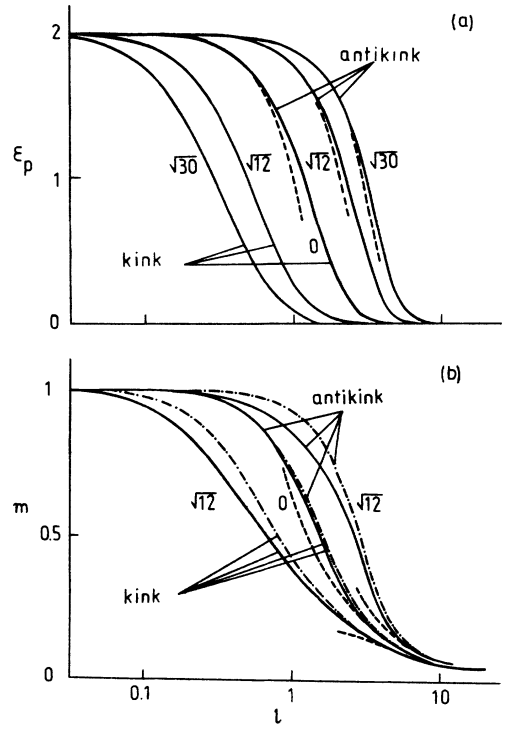

FIG. 5. The Peierls potential height ε_p (a) and the effective mass m (b) for kink and antikink as functions of the parameter l for the case of interaction of nearest neighbors only ($N^*=1$) for exponential law (1.2) at various values of the anharmonicity parameter β: $\beta\to 0$ (harmonic potential), $\beta=\sqrt{12}$, and $\beta=\sqrt{30}$. (b) shows effective masses calculated at the minimum $X=0$ (solid lines) as well as at the maximum $X=\pi$ (dash-dotted line) of the Peierls potential. In addition, dashed lines show calculations for weak-bond [(4.1), (4.3), and (4.11)–(4.13)] and continuum [(4.35) and (4.36)] approximations. Numerical simulation parameters: $\Theta_0=1$, $M=20$, $r=0$.

The calculation results are thus as follows: (1) the Peierls potential $\varepsilon(X)$ and its characterizing parameters ε_p and r_p; (2) effective kink mass $m(X)$; (3) pair creation energy $\varepsilon_{\text{pair}}$; and (4) kink interaction energy, determined from dependence $E_\sigma(Q)$ [see (2.16)].

It should be emphasized that the parameters calculated with the described computer technique correspond to the kink motion on the background of a commensurate structure with coverage Θ_0 and not with Θ. The distortion of kink characteristics due to interaction between kinks in the periodic structure of kinks at the selected calculation parameters ($M \gtrsim 20$) is negligible (see Sec. VI). Note, however, that the proposed method for calculating the kink mass m and parameter r_p of the Peierls potential is not rigorous because these characteristics are found from trajectory of the kink state which connects the saddle and the minimum points of energy surface (2.3), $E = V(x_1, x_2, \ldots, x_N)$, along a line whose points are determined from the solution of a set of $N-1$ algebraic equations:

$$\nabla_k V = 0, k \neq j_{\text{st}} . \tag{3.7}$$

For a rigorous calculation of the above-specified parameters, a "saddle" trajectory should be calculated which connects the saddle and the minimum points along the line of most rapid descent and is determined by the solution of a set of N differential equations

$$\frac{dx_k}{d\tau} = -\nabla_k V . \tag{3.8}$$

The principal results of the numerical simulations are shown in Figs. 5–11, where dependences of the preceding

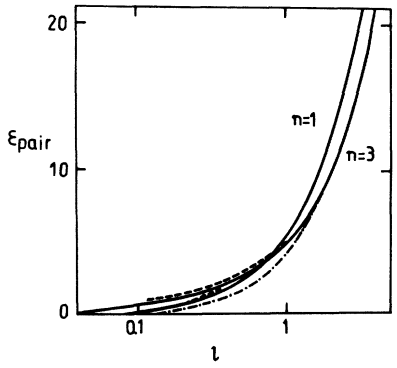

FIG. 7. Kink-antikink pair creation energy as a function of the parameter l for the Coulomb ($n=1$) mechanism of interaction at $\Theta_0=1$ and for the dipole ($n=3$) mechanism with coverages $\Theta_0=1$ (solid line) and $\Theta_0=\frac{1}{2}$ (dash-dotted line). Dashed lines show results of calculations in the weak-bond approximation. Calculation parameters are the same as for Figs. 6 and 8.

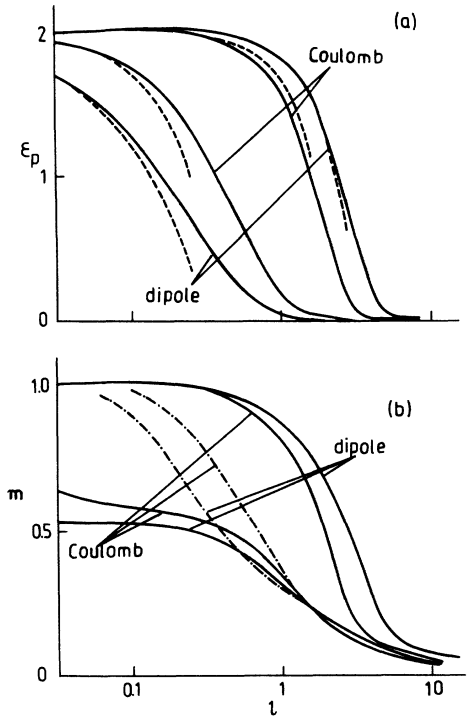

FIG. 6. Dependences $\varepsilon_p(l)$ (a) and $m(l)$ (b) for a kink and antikink for Coulomb and dipole mechanisms of particle interaction. Dash-dotted lines in (b) correspond to the effective mass at $X=\pi$. Dashed lines in (a) show results of calculations in the weak-bond approximation. Calculation parameters: $\Theta_0=1$, $M=20$, $r=0$, $N^*=1.7N$.

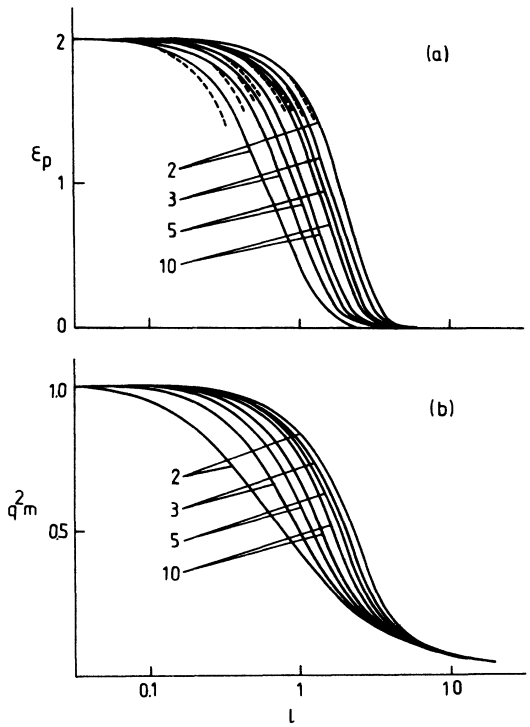

FIG. 8. Peierls potential height (a) and effective mass at $X=0$ (b) for a kink and antikink as functions of parameter l for the dipole interaction of adatoms at various coverages $\Theta_0=1/q$ ($q=2$, 3, 5, and 10). Curves are enumerated by index q. Dashed lines designate the weak-bond approximation. (b) shows dependences for q^2m to reduce $m(l)$ curves to the same scale.

kink characteristics on the magnitude of interaction between adatoms are presented. For convenience, the dependences are presented as functions of parameter l, introduced by analogy with the SG equation:

$$l=\pi[v''(a_A)]^{1/2}\ , \tag{3.9}$$

so that for the exponential potential of adatom interaction, (1.2), we have

$$l=(\beta/2)V_0^{1/2}\exp[-(\beta/2)(a_A/a_s-1)]\ , \tag{3.10}$$

and for the power law (1.3),

$$l=\tfrac{1}{2}\Theta_0^{n/2+1}[V_0 n(n+1)]^{1/2}\ . \tag{3.11}$$

Note also that a logarithmic scale on the abscissa axis is used in Figs. 5–11.

The present study investigates only the case of a repulsive interaction of atoms in a chain, when the function $v(x)$ and the atomic interaction forces decrease monotonically with the distance between atoms. The latter breaks the symmetry between a kink and an antikink, inherent in the classical FK model with a harmonic interaction potential (1.1). Namely, effective interaction forces for a kink (in a region of a local contraction) should exceed those for an antikink (in the region of a local extension of an atomic chain). Because of this, at the same value of parameter V_0 (or l), a kink, as compared with an antikink, should be characterized by lower values of the effective mass and Peierls potential height. These qualitative considerations are substantiated by Fig. 5 presenting the results of calculation of dependences $\varepsilon_p(l)$ and $m(l)$ for the FK model when interaction only between nearest atoms is taken into account, but at the same time, in contrast to the classical FK model, the interaction follows exponential law (1.2). It is seen that the splitting of curves in Fig. 5 is growing with the value of β.

Figure 6 shows dependences $\varepsilon_p(l)$ and $m(l)$ for the

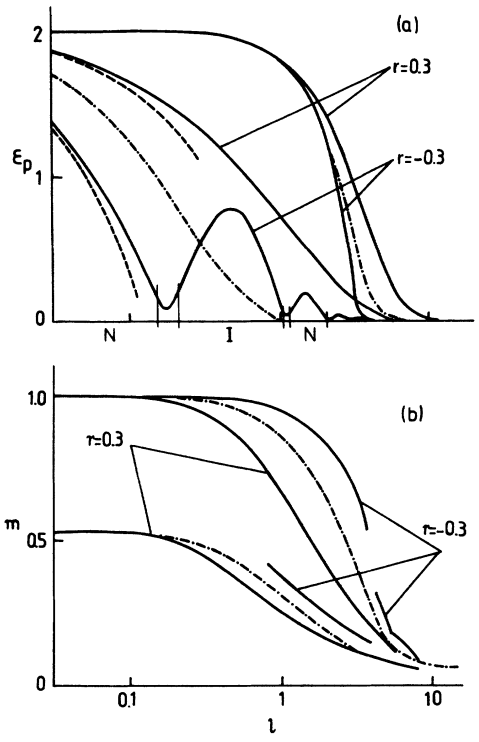

FIG. 10. Dependences $\varepsilon_p(l)$ (a) and $m(l)$ (b) at coverage $\Theta_0=1$ ($M=20$, $N^*=1.7N$) at the dipole interaction of atoms for the nonsinusoidal substrate potential (1.4) with parameter $r=\pm 0.3$. For comparison, dash-dotted lines show kink characteristics for the sinusoidal potential ($r=0$). The dashed lines show results of the weak-bond approximation.

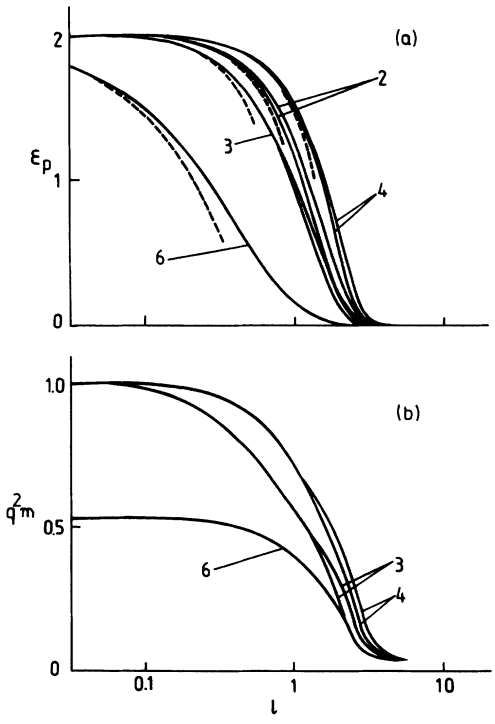

FIG. 9. Dependences $\varepsilon_p(l)$ (a) and $m(l)$ (b) for dipole interaction of atoms for the complex unit cell with coverage $\Theta_0=p/5$ ($p=2$, 3, 4, and 6). Curves are enumerated with index p; other designations are similar to Figs. 7 and 8.

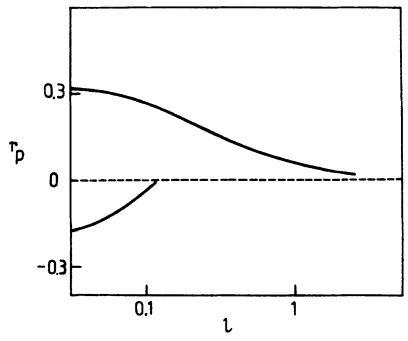

FIG. 11. Parameter r_p, characterizing the shape of kink potential relief $\varepsilon(X)$, as a function of parameter l for various shapes of substrate potential relief, $r=\pm 0.3$ ($n=3$), $\Theta_0=1$, $M=20$, $N^*=1.7N$).

long-range mechanisms [Coulomb ($n=1$) and dipole ($n=3$)] of adatom interaction. As can be seen, the dependences are qualitatively similar to those in Fig. 5. The difference between the parameters ε_p and m for a kink and an antikink at the same value of the parameter l for the dipole interaction, is much greater than for the Coulomb one, which is accounted for by a higher value of the anharmonicity of the dipole potential (see Sec. IV). No peculiar qualitative features are exhibited also by dependences $\varepsilon_{\text{pair}}(l)$ (Fig. 7).

Figure 8 shows dependences of kink and antikink parameters for a dipole interaction of atoms at different coverages $\Theta_0=1/q$ ($q=2$, 3, 5, and 10) having a simple unit cell. As seen, the difference between kink and antikink parameters decreases with increasing q (right down to zero at $q\to\infty$); this behavior can be explained by a corresponding decrease in the value of anharmonicity of the atomic interaction potential (see Sec. IV).

The next figure (Fig. 9) presents the same kink prameters for complex unit cells with coverage $\Theta_0=p/q$, $p>1$. It is seen that as the number of atoms in the unit cell, p, increases, the separation of dependences $\varepsilon_p(l)$ and $m(l)$, corresponding to a kink and an antikink, diminishes so that, e.g., for $\Theta_0=\frac{6}{5}$ ($p=6$) it becomes negligible. Such a behavior of plots in Fig. 9 is due to that, as will be shown in Sec. IV, interaction between adjacent unit cells rather than between adjacent atoms in one cell is responsible for the splitting of kink and antikink characteristics. Therefore, e.g., while the difference between kink and antikink parameters for coverage $\Theta_0=1$ is due to an anharmonicity of interaction potential at a characteristic distance $a_s=2\pi$, the difference for coverage $\Theta_0=1.2$ is caused by an anharmonicity of interaction at distance $5a_s=10\pi$, which obviously is much weaker.

Finally, Figs. 10 and 11 present the results of calculations for the case of a nonsinusoidal substrate potential (1.4). It is, first of all, seen from Fig. 10(b) that, as for the standard FK model[13] (see Fig. 2), a departure of the substrate potential shape from a sinusoidal one changes the effective kink mass: it increases at $r<0$ and decreases at $r>0$. Naturally, potential energy of the kink $\varepsilon(X)$ changes as well. Function $\varepsilon(X)$ has generally a minimum for the arrangement of atoms, shown in Fig. 4(a), and a maximum for the configuration in Fig. 4(c). We will conventionally call this situation the case of N (i.e., normal) relief. For the N relief it is convenient to approximate roughly the function $\varepsilon(X)$ by the Peyrard-Remoissenet function (1.4) (Ref. 13) with some parameters ε_p and r_p. It is obvious that $r_p\to r$ at $V_0\to 0$; calculations demonstrate (see Fig. 11) that as the V_0 value increases, parameter r_p approaches zero. The case of $r>0$ always corresponds to the N relief; in this case the ε_p values for both a kink and an antikink exceed corresponding ε_p values for a sinusoidal relief ($r=0$) [see Fig. 10(a)]. The case of $r<0$, when the potential $v_s(x)$ has the shape of narrow wells separated by broad gently sloping barriers, is more difficult. Apart from the N relief, an I (i.e., inverse) relief, where the configuration of Fig. 4(a) corresponds to a maximum, and of Fig. 4(c), to a minimum of function $\varepsilon(X)$, can also occur at certain parameter values in this case. As the energy of interaction of atoms in the chain increases, the cases of the N and the I relief become alternating [see Fig. 10(a)], and dependence $\varepsilon_p(l)$, similarly to the standard FK model,[13,36] becomes nonmonotonic. In addition, between N- and I-relief regions there exist intermediate regions [in Fig. 10(a) the N- and I-relief regions are marked by letters N and I] where the two configurations of Figs. 4(a) and 4(c) correspond to local maxima of function $\varepsilon(X)$, while its minimum occurs at some intermediate configuration [Fig. 4(b)] with $0<X<\pi$.[13] Dependence $\varepsilon_p(l)$ in the intermediate regions has pronounced local minima [see Fig. 10(a)]. The described features of function $\varepsilon_p(l)$ may substantially affect dynamical characteristics of the FK model (see Sec. VII).

IV. LOCAL MODEL

Firstly, we consider the cases where it suffices to take into account interaction of nearest neighboring atoms only.

A. Weak-bond approximation

It is most simple to consider a case where interaction between atoms is small ($V_0\ll\varepsilon_A$), so that all atoms are situated near corresponding minima of the substrate potential. For instance, at a coverage $\Theta_0<1$, when not more than one atom is at one adsorption well, small displacements of atoms form their positions corresponding to minima of the potential $v_s(x)$ can be neglected in the first approximation with respect to V_0. Then for the motion of kinks or antikinks on the background of the coverage $\Theta_0=p/q$ lying within the interval $(1+s)^{-1}<\Theta_0<s^{-1}$ [including a kink on the background of the coverage of $(1+s)^{-1}$ and an antikink on the background of s^{-1}], where $s\equiv\text{int}(\Theta_0^{-1})$ is an integer, from simple geometric considerations (see Figs. 3 and 4) we obtain ($a_s=2\pi$):

$$\varepsilon_p\simeq 2+2v(2\pi s+\pi)-v(2\pi s)-v(2\pi s+2\pi)\ . \tag{4.1}$$

It is important to note that in the same approximation the effective kink mass m (2.11), the kink-antikink pair creation energy $\varepsilon_{\text{pair}}$, and the difference of Peierls potential amplitudes for a kink and an antikink, $\delta\varepsilon_p$, depend only on the size of the unit cell a:

$$m\simeq 1/q^2\ , \tag{4.2}$$

$$\varepsilon_{\text{pair}}\simeq[v(a-2\pi)-v(a)]+[v(a+2\pi)-v(a)]\ , \tag{4.3}$$

$$\delta\varepsilon_p\simeq[2v(a+\pi)-v(a)-v(a+2\pi)] -[2v(a-\pi)-v(a-2\pi)-v(a)]\ . \tag{4.4}$$

For a harmonic potential of interaction between atoms it follows from (4.3) and (4.4) (Ref. 18) that for an arbitrary adatom concentration Θ_0,

$$\varepsilon_{\text{pair}}\simeq 4l^2,\quad \varepsilon_p\simeq 2-l^2,\quad \delta\varepsilon_p=0\ . \tag{4.5}$$

At a weak anharmonicity of the adatom interaction potential, $\beta\ll 1$, where

$$\beta \equiv -a_s v'''(a)/v''(a) , \tag{4.6}$$

expanding the potential $v(x)$ into a Taylor series, we obtain from (4.3) and (4.4)

$$\varepsilon_{\text{pair}} \simeq 4\mu l^2 , \tag{4.7}$$

$$\delta\varepsilon_p \simeq \beta\mu l^2 , \tag{4.8}$$

where $\mu \equiv v''(a)/v''(a_A)$ and $l=\pi[v''(a_A)]^{1/2}$ according to the definition (3.9). For a simple unit cell $\mu=1$, while for a complex one μ decreases rapidly with increasing number p of atoms in the unit cell:

$$\mu=\exp[-(\beta/\Theta_0)(p-1)]$$

for the exponential (1.2) and $\mu=p^{-(n+2)}$ for the power-law (1.3) potential. Hence, dependence of the Peierls potential amplitude on the coverage Θ_0 is similar to the "devil's staircase" (see Ref. 32 and Sec. VI): it exhibits jumps of $\delta\varepsilon_p$ in size at each rational coverage $\Theta_0=p/q$. Note that for the power-law potential (1.3), the paramenter $\beta=(n+2)/q$ describing the anharmonicity of the potential diminishes with decreasing of the coverage $\Theta_0=1/q$.

The case of a coverage $\Theta_0>1$ is somewhat more complex. Thus, in the ground state, for a kink on the background of $\Theta_0=1$ two atoms with coordinates x_1 and x_2 are situated in one well of the substrate potential (see Fig. 4) and their coordinates are $x_{1,2}=\pm x$, where the value $x \ll 1$ is determined from the solution of the linearized equation of motion:

$$\omega_0^2 x + v'(2x)=0 . \tag{4.9}$$

For the power-law potential (1.3), it follows from (4.9) that

$$x \simeq \pi[(2nV_0)/(2\pi\omega_0)^2]^{1/(n+2)} . \tag{4.10}$$

so that the ground-state energy is

$$E(0) \simeq \left[1+\frac{2}{n}\right](\pi\omega_0)^2 \left[\frac{2nV_0}{(2\pi\omega_0)^2}\right]^{2/(n+2)} , \tag{4.11}$$

with

$$\varepsilon_{\text{pair}} \simeq E(0) \tag{4.12}$$

and

$$\varepsilon_p \simeq 2-E(0) . \tag{4.13}$$

It is obvious that in the first approximation the amplitude of the Peierls potential is constant for kinks and antikinks on the background of any coverage Θ_0 within a range of $1<\Theta_0<\frac{3}{2}$.

The limit of applicability of the weak-bond approximation can be determined with the help of Figs. 5–10, where corresponding approximate dependences are plotted by dashed lines; the limit amounts to $l \lesssim 0.2$ for kinks and $l \lesssim 2$ for antikinks.

B. Continuum approximation

Let us now consider the case where interaction of adatoms along a chain is strong as compared with the substrate potential ($V_0 \gg \varepsilon_A$). Relative displacements of adatoms of the chain are then small [$u_x \cong (u_{j+1}-u_j)/a \ll 1$] so that the continuum approximation can be used.

If interaction $v(x)$ between adatoms decreases rapidly with the distance x at $x>a$ [e.g., according to the exponential law (1.2) with $\beta \gg 1$], then it suffices to take into account interaction only between the nearest neighbors. For a simple unit cell ($p=1$), when $\Delta=0$, equations of motion

$$\frac{d^2}{dt^2}u_j + \sin u_j + v'(a+u_j-u_{j-1}) - v'(a+u_{j+1}-u_j)=0 \tag{4.14}$$

follow from the Hamiltonian (2.1). Expanding the potential $v(x)$ into a Taylor series,

$$v'(a+u) \simeq v'(a)+v''(a)u+\tfrac{1}{2}v'''(a)u^2 , \tag{4.15}$$

we obtain from (4.14) [in general case $v'''(a) \neq 0$],

$$\frac{d^2}{dt^2}u_j + \sin(u_j) - v''(a)(u_{j+1}-2u_j+u_{j-1})\left[1+\frac{v'''(a)}{2v''(a)}(u_{j+1}-u_{j-1})\right]=0 . \tag{4.16}$$

Converting to a continuous variable $j \to x=ja$, $u_j \to u(x)$,

$$u_{j+1}-u_{j-1} \simeq 2au_x(x) , \tag{4.17}$$

$$u_{j+1}-2u_j+u_{j-1} \simeq a^2 u_{xx}(x)+\tfrac{1}{2}a^4 u_{xxxx}(x) , \tag{4.18}$$

we obtain

$$u_{tt}+\sin u - d^2\left[u_{xx}\left[1+\frac{av'''(a)}{v''(a)}u_x\right]+(a^2/12)u_{xxxx}\right]=0 , \tag{4.19}$$

where

$$d=a[v''(a)]^{1/2} \tag{4.20}$$

determines the kink "width." Note that d is related to the previously introduced parameter $l=\pi[v''(a_A)]^{1/2}$ for the coverage $\Theta_0=1/q$ by

$$d=a(l/\pi)=2lq . \tag{4.21}$$

Using a substitution

$$x=\tilde{x}d, \quad u(x)=\tilde{u}(\tilde{x}) , \tag{4.22}$$

we obtain the equation in a canonical form:

$$\tilde{u}_{tt}+\sin\tilde{u}-\tilde{u}_{\tilde{x}\tilde{x}}[1-\alpha\tilde{u}_{\tilde{x}}]-h\tilde{u}_{\tilde{x}\tilde{x}\tilde{x}\tilde{x}}=0 , \tag{4.23}$$

where the following designations are introduced [see also (4.6)]:

$$\alpha=-[av'''(a)]/[dv''(a)]=\beta/2l \tag{4.24}$$

and

$$h=a^2/12d^2=\pi^2/12l^2 . \tag{4.25}$$

The parameter h characterizes the effect of discreteness of the chain on the dynamics of the FK model; the term $\sim h$ exists also in the case of harmonic interaction potential $v(x)$ (1.1). The parameter α describes a weak departure of the potential $v(x)$ from the harmonic form (1.1).

If $\alpha=0$ and $h=0$, then the static kink-type solution of Eq. (4.23) has the well-known form (see, e.g., Ref. 5):

$$\tilde{u}_{\rm SG}(\tilde{x})=4\tan^{-1}\exp(-\sigma z), \quad z=\tilde{x}-X/d . \tag{4.26}$$

This solution describes an excitation which is characterized by the effective mass

$$m_{\rm SG}=8/ad=2/(\pi q^2 l) , \tag{4.27}$$

and corresponds to the following kink-antikink pair creation energy:

$$\varepsilon_{\rm pair}^{\rm (SG)}=16(d/a)=16(l/\pi) . \tag{4.28}$$

At small α and h, the solution of Eq. (4.23) can be obtained with the aid of the perturbation theory (see, e.g., Ref. 40):

$$\tilde{u}(\tilde{x})=u_{\rm SG}+u_{\alpha}+u_{h} , \tag{4.29}$$

$$u_{\alpha}=(4\alpha/3\cosh z)\tan^{-1}(\sinh z) , \tag{4.30}$$

$$u_{h}=\sigma h\left[\frac{1}{\cosh z}\right](z-3\tanh z) . \tag{4.31}$$

A simple analysis shows that discreteness effects described by the parameter h ($h>0$) result in a kink narrowing[20] since $d\to d_{\rm eff}=d(1-h/2)$; later we will neglect this effect. The anharmonicity of interaction between adatoms (i.e., the term $\sim\alpha$) violates the symmetry between a kink and an antikink since, according to (4.30), the correction u_{α} is independent of σ. This means that the effective kink width changes by an amount of $\sigma\alpha(\pi d/3)$, i.e., at $\alpha>0$ the effective width of the kink ($\sigma=+1$) increases, and of the antikink ($\sigma=-1$), decreases. This leads to the corresponding difference in other parameters characterizing the kink and antikink.

Substituting the function

$$u_j\simeq\tilde{u}\{(\pi/l)[j-(X/a)]\} \tag{4.32}$$

into formulas (2.9), (2.11), and (2.17) and using, similarly to Ref. 21, the Poisson summation rule, we obtain, approximately,

$$\varepsilon_{\rm pair}\simeq\sum_{\sigma=-1}^{+1}\sum_{j}\{(1-\cos u_j^{\sigma})+\tfrac{1}{2}(l/\pi)^2(u_{j+1}^{\sigma}-u_j^{\sigma})^2[1-(\alpha l/3\pi)(u_{j+1}^{\sigma}-u_j^{\sigma})]\}$$
$$\simeq\varepsilon_{\rm pair}^{\rm (SG)}\left[1-\frac{4\alpha^2}{27}\right] , \tag{4.33}$$

$$m(X)\simeq m+\tfrac{1}{2}(\Delta m)\cos(X/q) , \tag{4.34}$$

$$m=\tfrac{1}{8}m_{\rm SG}\int_{-\infty}^{+\infty}dx[\tilde{u}_x(x)]^2\simeq m_{\rm SG}\left[1-\frac{\pi}{6}\sigma\alpha\right] , \tag{4.35}$$

$$\Delta m=\tfrac{1}{2}m_{\rm SG}\int_{-\infty}^{+\infty}dx[\tilde{u}_x(x)]^2\cos(2lx)$$
$$\simeq\frac{4m_{\rm SG}l}{\sinh(\pi l)}-\frac{16\alpha\sigma}{3}\left[\frac{\pi(4l^2+1)}{4\cosh(\pi l)}+l\int_{-\infty}^{+\infty}\frac{dz}{\cosh^2 z}\tan^{-1}(\sinh z)\sin(2lz)\right]$$
$$\approx 8\left[m_{\rm SG}-\frac{\alpha\sigma}{3}\pi(\pi+2)l\right]le^{-\pi l}, \quad l\to\infty . \tag{4.36}$$

$$\varepsilon(X)=\int dX\frac{\partial E}{\partial X}=\int dX\sum_{j}\frac{\pi^2}{12dl^2}\tilde{u}_x\tilde{u}_{xxxx}(1-\alpha\tilde{u}_x)\simeq\tfrac{1}{2}\varepsilon_p\cos(X/q) , \tag{4.37}$$

$$\varepsilon_p=\frac{\pi}{6l^2}\int_{-\infty}^{+\infty}dx\,\tilde{u}_x\tilde{u}_{xxxx}[1-\alpha\tilde{u}_x]\sin(2lx)$$
$$\simeq\frac{8}{3}\frac{(\pi l)^2}{\sinh(\pi l)}\left[1+\frac{1}{2l^2}\right]\simeq\tfrac{16}{3}(\pi l)^2\exp(-\pi l) . \tag{4.38}$$

Thus, with identical parameters of the system, because of the anharmonicity of interaction potential, the kink is characterized by a greater (as against the antikink) effective width [see (4.30)], and hence by lower values of the Peierls potential and effective mass, the corresponding difference being proportional to the anharmonicity parameter α; e.g., for the mass,

$$\Delta m_p = m(\sigma=-1) - m(\sigma=+1) \simeq m_{\rm SG}\alpha\pi/3 \ . \quad (4.39)$$

Figure 5 presents a comparison of the results of numerical simulations for the case where only the nearest neighbors interact according to exponential law (1.2) with approximate expressions (4.34)–(4.38). As can be seen, at $l \gtrsim 5$ the continuum approximation agrees fairly well with the numerical results. Note that for the power-law potential (1.3) at a coverage $\Theta_0 = 1/q$ the parameters d and α are

$$d = \left[\frac{n(n+1)V_0}{q^n}\right]^{1/2}, \quad \alpha = (n+2)/d \ . \quad (4.40)$$

Hence, for the fixed parameter l, the anharmonicity parameter α (and, therefore, the difference between antikink and kink characteristics) descreases with both decreasing exponent n and increasing unit cell size q, which is confirmed by numerical calculation results (see Sec. III).

As distinct from the case of a simple unit cell, the case of $p \geq 2$ is essentially more complicated. For example, at $p=2$ the continuum approximation leads to the so-called double SG equation (see details in Appendix A and Ref. 41). For example, to calculate the values of $\varepsilon_{\rm pair}$ and $\delta\varepsilon_p$ in this case the interaction between p nearest neighbors should be taken into account as minimum.

Taking into account the interaction of all atoms in the chain (not only between the neighboring ones) for the exponential law (1.2) leads to the local SG equation (4.23) also. However, as it is shown in Appendix B with the help of the method of Refs. 42 and 43, the parameters of this equation are modified:

$$d \to d_{\rm eff} = d(1+S+S/J)^{1/2}(1-S)^{-3/2} > d$$

and

$$\alpha \to \alpha_{\rm eff} = \alpha(d/d_{\rm eff})^3 < \alpha \ ,$$

where $J \equiv (d/2\pi)^2(1-S)^{-1}$ and $S \equiv \exp(-\beta)$.

V. NON-LOCAL MODEL

When not only the nearest neighbors interact with one another, but the potential $v(x)$ remains short range (e.g., exponential), the equations of motion in the continuum limit reduce again to a SG-type local equation with the kink parameter ($p=1$)

$$d \to d_{\rm eff} = a\left[\sum_{j=1}^{\infty} j^2 v''(ja)\right]^{1/2} . \quad (5.1)$$

However, for a long-range interaction potential, such as a power-law one (1.3), the continuum limit results in an integro-differential equation (see Ref. 44). To derive the equation for the case of a simple unit cell ($\Theta_0 = 1/q$), we use a continuous variable $j \to y = ja$, $\sum_j \to \int dy/a$. Next, we change the variable: $y \to x = y + u(y)$, so that approximately,

$$\begin{aligned} dx &= [1+u_y(y)]dy \simeq [1+u_x(x)]dy \ , \\ dy &\simeq [1-u_x(x)]dx \ . \end{aligned} \quad (5.2)$$

Then the adatom interaction energy takes the form

$$H_{\rm int} = \tfrac{1}{2}\sum_{j\neq j'} v(x_j - x_{j'}) \to \tfrac{1}{2}\int\int \frac{dx\,dx'}{a^2}[1-u_x(x)][1-u_{x'}(x')]v(x-x') \ . \quad (5.3)$$

Discarding insignificant constant terms, we obtain

$$H_{\rm int} = \tfrac{1}{2}\int\int \frac{dx\,dx'}{a^2} u_x(x)u_{x'}(x')v(x-x') \ . \quad (5.4)$$

Expression (5.4) has a simple physical meaning, since the value

$$\rho(x) = -u_x(x)/a \quad (5.5)$$

is the density of the excess (with respect to the initial commensurate structure) adatoms, so that

$$\int \rho(x)dx = \sigma/q \ . \quad (5.6)$$

For a local potential of atomic interactions,

$$v(x) = a\delta(x)d^2 \ , \quad (5.7)$$

expression (5.4) takes the form corresponding to the SG equation. For the nonlocal power-law potential (1.3) the integral (5.4) diverges at $x - x' \to 0$, and, therefore, the integration should be cut off at some distance a^*:

$$H_{\rm int} = \tfrac{1}{2}\int \frac{dx}{a}u_x(x)\int \frac{dx'}{a}u_x(x+x')v(x') \quad (5.8a)$$

$$\simeq \tfrac{1}{2}\int \frac{dx}{a}[u_x(x)]^2\left[\int_{-a^*}^{+a^*}\frac{dx'}{a}v(x')\right] + \tfrac{1}{2}\int \frac{dx}{a}u_x(x)\int_{a^*}^{\infty}\frac{dx'}{a}v(x')[u_x(x+x')+u_x(x-x')]$$

$$= \tfrac{1}{2}\int \frac{dx}{a}[u_x(x)]^2 d^2 + \tfrac{1}{2}V_0(2\pi)^n\int \frac{dx}{a}u_x(x)\int_{a^*}^{\infty}\frac{dx'}{a}\frac{1}{(x')^n}[u_x(x+x')+u_x(x-x')] \ . \quad (5.8b)$$

Introducing the dimensionless variables by the substitution $x = \bar{x}d$, we obtain the nonlocal Hamiltonian

$$H=\left[\frac{d}{a}\right]\int dx\left\{\frac{1}{2}[\tilde{u}_t(x)]^2+[1-\cos\tilde{u}(x)]+\tfrac{1}{2}[\tilde{u}_x(x)]^2+\tfrac{1}{2}A\tilde{u}_x(x)\int_{a^*/d}^{\infty}dx'(x')^{-n}[\tilde{u}_x(x+x')+\tilde{u}_x(x-x')]\right\}, \quad (5.9)$$

where

$$A\equiv\frac{V_0}{(2\pi)^2q^{n+2}}\left[\frac{a}{d}\right]^{n+1}. \quad (5.10)$$

If the potential $v(x)$ were short-range, then, without the second term in equation (5.8b), the expression for the energy would take the form of the corresponding expression of the SG system, for which, according to (4.20),

$$d^2=V_0n(n+1)/q^n. \quad (5.11)$$

We use this relation to reduce the quantity of independent variables and express the parameter V_0 of the potential (1.3) in terms of the parameter d. As a result,

$$A=\alpha^{n-1}/n(n+1),\quad \alpha=a/d=\pi/l. \quad (5.12)$$

It is also natural to take $a^*=a$; and the Hamiltonian (5.9) will be a function of only two parameters, α and n.

The motion equation corresponding to the Hamiltonian (5.9) is

$$\tilde{u}_{tt}-\tilde{u}_{xx}+\sin\tilde{u}=A\frac{\partial}{\partial x}\int_{\alpha}^{\infty}dx'(x')^{-n}[\tilde{u}_x(x+x')+\tilde{u}_x(x-x')], \quad (5.13)$$

which describes the dynamics of a chain with a nonlocal interaction having an amplitude A in the continuum approximation. To find the kink-type static solution, the solution of the equation of motion (5.13) at $u_{tt}=0$ with asymptotics

$$u(x\to+\infty)-u(x\to-\infty)=-2\pi\sigma$$

is to be determined. It is readily understood that such a solution does always exist, but its asymptotic, which is determined by the last term of (5.13), substantially differs from that of the SG kink and is a power-law one. Indeed, linearizing the equation (5.13) near the kink "tail" $u=u(|x|\to\infty)$ and integrating it by parts, we obtain approximately (see also Ref. 44),

$$|\tilde{u}(\tilde{x})-\tilde{u}(|\tilde{x}|=\infty)|\simeq 2\pi nA/|\tilde{x}|^{n+1},\quad x\to\infty. \quad (5.14)$$

To calculate the other characteristics of the kink in the nonlocal model, its shape should be numerically determined first.

If the system contains two kinks having topological charges σ_1 and σ_2 and separated by some long distance x_0 ($x_0\to\infty$), then in the zero approximation the solution of equation (5.13) can be represented as a superposition of two SG kinks (4.26):

$$\tilde{u}(\tilde{x},t)=\tilde{u}_{SG}^{(1)}(\tilde{x}-\tfrac{1}{2}\tilde{x}_0(t))+\tilde{u}_{SG}^{(2)}(\tilde{x}+\tfrac{1}{2}\tilde{x}_0(t)). \quad (5.15)$$

Within the framework of the adiabatic perturbation theory[40] the dependence of the relative coordinate x_0 on the time t is given by the following equations:

$$\frac{d\tilde{x}_0}{dt}=\tilde{v},$$
$$\frac{d\tilde{v}}{dt}=-\sigma_1\sigma_2A\int_{-\infty}^{+\infty}\frac{dz}{\cosh(z+\tilde{x}_0)}\int_{\alpha}^{\infty}\frac{dx'}{(x')^n}\left[\frac{\sinh(z+x')}{\cosh^2(z+x')}+\frac{\sinh(z-x')}{\cosh^2(z-x')}\right]. \quad (5.16)$$

At $x_0\to\infty$ this system leads to the equation

$$\frac{d^2\tilde{x}_0}{dt^2}=(2\pi)^2nA\sigma_1\sigma_2/\tilde{x}_0^{n+1}=-\partial\tilde{v}_{int}(x_0)/\partial\tilde{x}_0, \quad (5.17)$$

from which it follows that

$$\tilde{v}_{int}(\tilde{x})=(2\pi)^2A\sigma_1\sigma_2/\tilde{x}_0^{n}. \quad (5.18)$$

Returning to dimensional variables ($x=\tilde{x}d$, $v_{int}\equiv\tilde{v}_{int}/\alpha$), we obtain that the kink interaction is in the zero approximation described by expression (2.12) with

$$\tilde{V}_0=V_0/q^{n+2}, \quad (5.19)$$

which at $n=1$ coincides with previously derived relation (2.15). The next corrections to the law (2.12), caused by a power-law character of the shape of the kink "tails" (5.14), are as well power-law ones (see the next section).

The equation of motion (5.17) at $\sigma_1=-\sigma_2$ can be used for approximately describing the behavior of a large-amplitude breather. The first integral of equation (5.17) is trivial:

$$\varepsilon_{br}=\frac{1}{2}\left[\frac{d\tilde{x}_0}{dt}\right]^2+\tilde{v}_{int}(\tilde{x}_0)=\text{const}, \quad (5.20)$$

where $|\varepsilon_{br}|$ is the energy of coupling of the kink-antikink pair in the breather ($\varepsilon_{br}<0$). The breather oscillation period T and its frequency ω are determined by the following expressions:

$$T=\frac{2\pi}{\omega}=4\int_0^{x_{max}}\frac{dx}{2\pi\sqrt{2A}}\frac{1}{(x^{-n}-x_{max}^{-n})^{1/2}}=A^{-1/2}C_nx_{max}^{(1+n/2)},$$
$$C_n=\sqrt{2}\Gamma\left[\frac{1}{n}+\frac{1}{2}\right]\Big/\sqrt{\pi}\Gamma\left[\frac{1}{n}\right], \quad (5.21)$$

where x_{max} is the amplitude of the breather oscillations:

$$x_{\max}=[(2\pi)^2 A/|\varepsilon_{\rm br}|]^{1/n}\sim\omega^{-2/(n+2)} . \quad (5.22)$$

From equations (5.21) and (5.22) it follows that

$$|\varepsilon_{\rm br}|=(C_n\omega)^{2n/(n+2)}/(4\pi^2 A)^{2/(n+2)} . \quad (5.23)$$

It should be remembered that relations $x_{\max}\sim|\ln\omega|$ and $|\varepsilon_{\rm br}|\sim\omega^2$ hold in the local FK model, which formally corresponds to the limit $n\to\infty$ for the nonlocal FK model.

VI. INTERACTION OF KINKS. RENORMALIZATION

It was shown earlier [see (2.12) and (5.19)] that for a long-range interaction between adatoms with the power law (1.3), interaction of kinks should also be described by the similar law,

$$v_{\rm int}^{(0)}(x)=\tilde{V}_0/|x/a|^n,\quad \tilde{V}_0=V_0/q^{n+2} . \quad (6.1)$$

Expression (6.1), however, does not take into account that kinks are "soft" (deformable) quasiparticles. The mutual influence of kinks on one another changes their shapes and leads to the contribution to the system energy, which can be interpreted as an additional interaction $v_{\rm int}(x)$ between kinks. It is obvious that at long distances the behavior of this interaction $v_{\rm int}(x)$ will be governed by the asymptotics of the kink shape:

$$v_{\rm int}(x)\sim u_x(x) \quad (6.2)$$

[it will be recalled that $u_x(x)$ is proportional to the density of "excess" adatoms, see (5.5)]. For example, for the SG equation it was derived in Ref. 45 that

$$v_{\rm int}^{(\rm SG)}(x)=\frac{32l}{\pi}\exp(-x/d) . \quad (6.3)$$

From the kink asymptotics (1.6) for a nonsinusoidal potential of the substrate it follows that $v_{\rm int}>v_{\rm int}^{(\rm SG)}$ at $r>0$, and for $r<0$, $v_{\rm int}<v_{\rm int}^{(\rm SG)}$.

The effect of chain discreteness on the interaction between kinks for the standard FK model was numerically studied in Ref. 18, where the exponential law of kink interaction

$$v_{\rm int}^{(\rm FK)}(x)=A\exp(-\gamma x/d) \quad (6.4)$$

was shown to be valid at $x\gtrsim 3a$ and at any values of the parameter l, although the coefficients A and γ at $l\lesssim 5$ depend on l (see Fig. 12); in particular, at $l\to 0$, $A(l)\simeq 4l^2$.

Using relation (6.2), it is easy to predict the change in the kink interaction asymptotics in the case of a short-range interaction of atoms because of anharmonicity of the interaction potential (see Sec. IV) and departure of the substrate potential relief shape from the sinusoidal shape (see Sec. I). For the long-range interaction potential (1.3) the relation (6.2) and asymptotics (5.14) predict the following dependence:[44]

$$v_{\rm int}(x)\sim x^{-(n+2)} . \quad (6.5)$$

For a numerical study of the function $v_{\rm int}(x)$, the energy (2.16) of a kink lattice per one kink should be calculated. The change in the kink energy, $\Delta E_\sigma(Q)$, with the distance between kinks, $x=Qa$, can be interpreted as the result of their pair interaction:

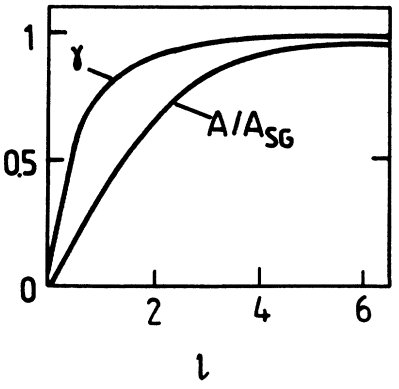

FIG. 12. The ratio $A/A_{\rm SG}$ [$A_{\rm SG}=32(l/\pi)$] and the parameter γ which determines, according to (6.4), kink interaction in the FK model, as functions of parameter l. The numerical data are taken from Ref. 18.

$$\Delta E_\sigma(Q)=E_\sigma(Q)-E_\sigma(\infty)\simeq\tfrac{1}{2}\sum_{j=-\infty}^{\infty}{}' v_{\rm int}(jaQ) . \quad (6.6)$$

The calculation results are presented in Fig. 13. As can

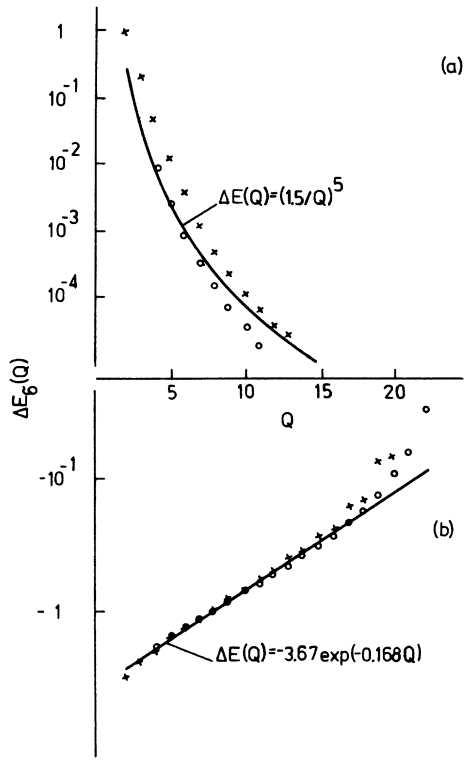

FIG. 13. The interaction energy of kinks as a function of the distance between them atomic for the dipole ($n=3$) (a) and the Coulomb ($n=1$) (b) mechanisms of atomic interaction in the chain. Results for the kink indicated by crosses, and for the antikink, by circles. Calculation parameters: $l=\pi/2$, $\Theta_0=1$, $r=0$.

be seen, within the studied range of variation of the distance x, interaction of kinks at a dipole interaction potential ($n=3$) is governed by the law $\Delta E_\sigma(Q) \sim Q^{-5}$, which agrees with the predicted expression (6.5). For the Coulomb potential ($n=1$), the calculation for the short-range region results in the dependence $\Delta E_\sigma(q) \sim -\exp(-\gamma Q)$ which resembles the law (6.4) for the SG equation, but differs from it both by the sign and by numerical coefficients. In the long-range region (at $Q \gtrsim 15$), where reaching the asymptotics $\Delta E \sim Q^{-3}$ can be expected, numerical calculations could not be conducted due to the restriction on the chain length ($N \sim 20$) caused by the limited computer time.

It is obvious that interaction between kinks, changing the kink shape, also changes its characteristics (the effective mass, the amplitude of the Peierls potential, etc.) for a simultaneous motion of the kink lattice. However, the calculation results demonstrate that the changes are small and can be fully neglected for distances $Q \gtrsim 3-5$.

The latter fact makes it possible to interpret complex structures of quasi-one-dimensional adsorbed layers with the help of a "renormalization" procedure.[46] Namely, suppose we needed to find characteristics of a kink on the background of some complex structure with a coverage $\Theta_1 = p_1/q_1$ and an interaction V_0 (so that parameter $R = V_0/\varepsilon_A = V_0/2$), when near the coverage Θ_1 there exists a simpler structure with a coverage $\Theta_0 = p_0/q_0 < \Theta_1$. With fixed Θ_0 and R, we first find from corresponding formulas or graphs (see Figs. 6–11 and Sec. IV) the effective kink mass $m^{(0)}$ and Peierls energy $\varepsilon_p^{(0)}$. Then, in accordance with (3.3), we treat the adatom structure with the coverage Θ_1 as a kink lattice on the background of the structure with the coverage Θ_0:

$$\frac{p_1}{q_1} = \frac{p_0}{q_0} + \frac{1}{Mq_0} = \frac{1}{q_0}\left[p_0 + \frac{1}{M}\right], \tag{6.7}$$

for which the distance between kinks is

$$Ma_s = Qa = Qq_0 a_s . \tag{6.8}$$

Thus, we obtain a commensurate lattice of quasiparticles whose masses are $m^{(0)}$, characterized by a coverage $\Theta_0 = 1/Q$ and placed into a periodic potential with an amplitude $\varepsilon_p^{(0)}$ and a period $a = qa_s$, interaction between the quasiparticles being determined by the law (6.1) with the parameter $\tilde{V}_0 = V_0/q_0^{n+2}$. Next, with given values of Θ_0 and $\tilde{R} \equiv \tilde{V}_0/\varepsilon_p^{(0)}$, we find once again the kink ("superkink") parameters $m^{(1)}$ and $\varepsilon_p^{(1)}$. Returning to the initial units, we obtain that the kink motion on the background of the structure with the coverage Θ_1 has the following parameters:

$$m = m^{(0)}m^{(1)}, \quad \varepsilon_p = \varepsilon_A(\varepsilon_p^{(0)}/2)(\varepsilon_p^{(1)}/2) . \tag{6.9}$$

When needed, the "renormalization" procedure can be repeated by the required number of times. It is, however, clear that the procedure provides an adequate accuracy only at great enough values of Q (i.e., at $\Theta_1 - \Theta_0 \ll \Theta_0$), when the corrections $v_{\text{int}}(x)$ to the kink interaction law (6.1) can be neglected. Note also that at a nonsinusoidal shape of the substrate potential, the parameter r is also subject to the "renormalization:" $r \to r_p^{(1)} \to \cdots \to r_p^{(m)}$, $r_p = r_p^{(m)}$.

Numerical calculations accompanied by the "renormalization" procedure allow us to obtain the dependence of the amplitude of the Peierls potential ε_p on the adatom concentration Θ at a constant parameter V_0 of the power law of adatom interaction. The results of the ε_p calculation for the dipole interaction law ($n=3$) at various values of the parameter V_0 are presented in Fig. 14. As can be seen, the function $\varepsilon_p(\Theta)$ undergoes jumps at every rational coverage Θ. The curve $\Theta(\varepsilon_p)$ is similar to the devil's staircase[32] (see also Sec. IV). From the results of the numerical calculation (Sec. III) as well as of an approximate analysis (Sec. IV), it follows that the jumps have the maximum amplitude at $l \cong 1$, where, according to (3.11),

$$l = \tfrac{1}{2}[n(n+1)V_0\Theta^{n+2}]^{1/2} .$$

The relative value of a jump decreases with both increasing period of the structure q and increasing number p of atoms in the unit cell.

The value of ε_p coincides with the diffusion activation energy (see Sec. VII), and, therefore, the devil's staircase should be directly observed in diffusion experiments.

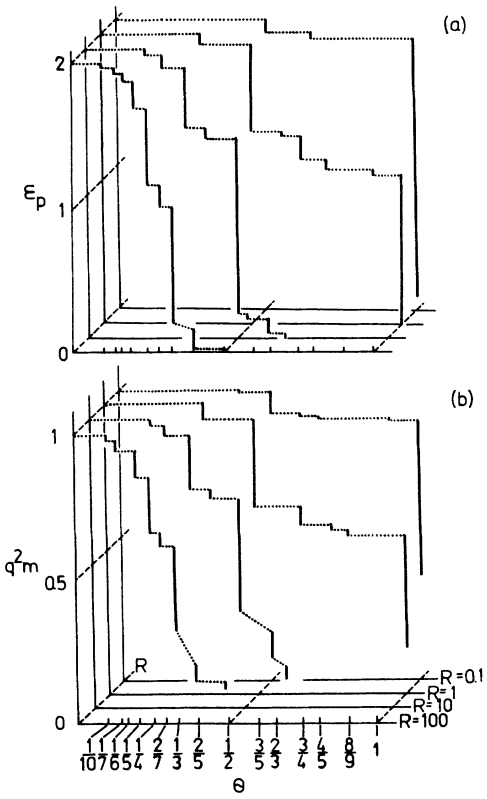

FIG. 14. Peierls energy ε_p (a) and the value mq^2 (b) as functions of coverage Θ for dipole interaction of atoms ($n=3$) at various values of the parameter $R \equiv V_0/\varepsilon_A$ ($R = 0.1$, 1, 10, and 100).

However, at the system temperature $T\neq 0$, the long-range order in a one-dimensional chain is impossible, and the correlation function

$$G(i-j)\equiv\langle u_i u_j\rangle-\langle u_i\rangle\langle u_j\rangle$$

decreases exponentially:

$$G(x)\sim\exp(-x/L)\ . \tag{6.10}$$

By analogy with the one-dimensional Ising model (see, e.g., Ref. 47), the correlation length L can be determined as the average distance between kinks and antikinks in the given structure:

$$L\simeq a_s/\Theta_{\rm pair},\quad \Theta_{\rm pair}\simeq\frac{1}{q}\exp(-\varepsilon_{\rm pair}/T)\ , \tag{6.11}$$

so that

$$L(\Theta,T)\simeq 2\pi q\exp[\varepsilon_{\rm pair}(\Theta)/T]\ . \tag{6.12}$$

For simple structures ($\Theta=1/q$), in accordance with (4.28) and (3.11), $\varepsilon_{\rm pair}\sim l\sim\Theta^{1+n/2}$, so that the correlation length decreases with decreasing concentration Θ. The results obtained in the framework of the weak bond and the continuum approximations (Sec. IV) demonstrate that $\varepsilon_{\rm pair}$ for complex structures ($p\geq 2$) is much less than for simple ones; due to this, the short-range order in complex structures gets destroyed at lower temperatures.

It is obvious that as long as for a given structure the kink's width is less than the correlation length [$d(\Theta)\ll L(\Theta;T)$], a jump of the function $\varepsilon_p(\Theta)$ is approximately temperature independent and equal to the corresponding jump at $T=0$. When the temperature is increased above $T_c(\Theta)$, determined from the condition

$$d(\Theta)=L(\Theta;T_c)\ , \tag{6.13}$$

the amplitude of the jump starts decreasing right up to its disappearance. The temperature $T_c(\Theta)$ may be interpreted as a "melting" temperature of the structure with coverage Θ. Thus, the devil's staircase will smoothen with increasing temperature since only jumps at the coverages corresponding to simple commensurate structures ($\Theta=1$, $\frac{1}{2}$, etc.) will "survive."

It is clear that a similar structure is also exhibited by the dependence $q^2m(\Theta)$ [see Fig. 14(b)].

VII. ON DIFFUSION IN ONE-DIMENSIONAL ADSYSTEMS

Thus, a kink in the considered system can be approximately treated as a quasiparticle of mass m, having the coordinate X and placed into the effective periodic potential

$$\varepsilon(X)\simeq\tfrac{1}{2}\varepsilon_p\frac{(1-r_p)^2[1-\cos(2\pi X/a)]}{[1+r_p^2+2r_p\cos(2\pi X/a)]}\ , \tag{7.1}$$

small oscillations of the kink ($X\ll a$) near potential relief minima being characterized by the frequency

$$\omega_p=\frac{1-r_p}{1+r_p}\left[\frac{\varepsilon_p}{2mq^2}\right]^{1/2}\ . \tag{7.2}$$

When the system parameters change, ε_p and mq^2 change "in step" (see Figs. 5, 6, 8, 9, and 14), and, therefore, ω_p should in this case change insignificantly near the value of $\omega_p\sim 1$.

The above-calculated kink characteristics correspond to its adiabatic (i.e., infinitely slow) motion. Naturally, at a kink motion with a nonzero velocity the characteristics may somewhat differ from the calculated ones. In addition, as pointed out in the Introduction, a departure from an exact integrability results in radiative losses of the kinetic energy of the kink at its motion; the latter effect can be approximately characterized by some "internal" friction coefficient η in Refs. 5 and 19–21.

The model considered in the present paper ignored the important fact that the external periodic potential for adatoms is formed by substrate atoms which are not stationary. The account of this fact leads to three consequences. *Firstly*, substrate atoms can shift from their equilibrium positions and "adapt" themselves to adatoms ("polaronic" effect). *Secondly*, oscillations of substrate atoms at $T\neq 0$ result in "smoothening" of the substrate potential (the Debye-Waller effect). Note that these two effects lead to a renormalization of the system parameters ε_A and r and should be automatically taken into account at their determination from experimental data (see Sec. I). *Thirdly*, interaction between moving adatoms and substrate atoms gives rise to an energy exchange between them and hence to an additional mechanism of energy loss ("external" friction) at a kink motion. Performing the operation $mq\sum_{k=-\infty}^{\infty}\cdots$ for both sides of the equation of motion (3.4) and taking into account the definition (2.8) of the kink coordinate X, one will readily see that the coefficient of "external" friction for the kink motion coincides with the coefficient of friction for an individual adatom. The calculation of the rate of the energy exchange at oscillations of single adatoms with some frequency ω_0 yields the following values:[48–51] $\eta_{\rm ex}\sim 10^{-2}\omega_0$ at oscillations of light (as compared with the substrate atom mass) and $\eta_{\rm ex}\lesssim\omega_0$ at motions of heavy adatoms. The estimates of Ref. 37 indicate that it is the "external" friction mechanism which is the main one for adsystems.

It would be natural to expect that with the account of expressions (2.10) and (2.9) for the kinetic and the potential energy of the kink and also with allowance for friction forces ($\eta=\eta_{\rm in}+\eta_{\rm ex}$) the kink motion at a nonzero substrate temperature ($T\neq 0$) will be adequately described be the Langevin equation:

$$m\frac{d^2X}{dt^2}+m\eta\frac{dX}{dt}+\partial\varepsilon(X)/\partial X=F(t)\ , \tag{7.3a}$$

$$\langle F(t)F(0)\rangle=2\eta mT\delta(t)\ . \tag{7.3b}$$

This assumption is confirmed by numerical experiments[52] conducted by the molecular dynamics method. It follows from (7.3) that for times $t\gtrsim\eta^{-1}$ the kink motion should be diffusive with a diffusion coefficient:

$$D=D_0\exp(-\varepsilon_p/T),\quad D_0\equiv K_0b^2\ , \tag{7.4}$$

where at temperatures below "melting" temperature, $T<T_c(\Theta)$ [see Eq. (6.13)], the kink free path length b in

the case of intermediate friction ($\eta > 10^{-2}\omega_p$) is to be taken equal to the adatomic structure period $a = qa_s$, and the rate K_0 of the kink escape from a potential well is given by the Kramers theory:[53]

$$K_0 \simeq \omega_p/2\pi \quad \text{at } \eta \lesssim \omega_p^* ,$$

and

$$K_0 \simeq \omega_p \omega_p^*/2\pi\eta \quad \text{at } \eta \gtrsim \omega_p^* ,$$

where

$$\omega_p^* = \frac{1+r_p}{1-r_p}[\varepsilon_p/(2mq^2)]^{1/2} . \tag{7.5}$$

It is interesting that for rarefied structures with $\Theta = 1/q$ at a weak enough friction, $\eta \lesssim \omega_p^*$, it follows from (7.4) that

$$D_0 \simeq 2\pi\omega_p q^2 \sim \Theta^{-2} , \tag{7.6}$$

i.e., both the diffusion activation energy and, owing to an increase of the free path length, the preexponential factor increase simultaneously with decreasing concentration (the so-called compensation effect[10]). Note, however, that the value of $T_c(\Theta)$ decreases simultaneously with Θ, so that structures with large enough periods will be destroyed due to thermal fluctuations. It is obvious that the usual relation $D_0 \simeq T/m\eta$ should hold true at high enough temperatures, $T \gg \varepsilon_p$. From the dependences $\varepsilon_p(\Theta)$ and $q^2 m(\Theta)$, determined in the preceding section (see Fig. 14) it follows that the dependence $D(\Theta)$ should have jumps similar to the devil's staircase: the value of D should rise sharply whenever the concentration Θ exceeds the Θ_0 value that characterizes a structure commensurate with the substrate, having at a given T a correlation length L that exceeds the kink width d.

Since the concentration of kinks in a chain is linearly proportional to the concentration of adatoms, the coefficient of diffusion of kinks coincides with the coefficient of "chemical" diffusion of adatoms.[10] For adsystems the parameter $R = V_0/\varepsilon_A$ is generally within 0.1–10. Namely, for the Coulomb repulsion of adatoms ($n = 1$), $R = e^2 R_0$, where $R_0 = (a_s \varepsilon_A)^{-1}$ (taking $a_s \simeq 3$ Å for a tungsten substrate and $\varepsilon_A \simeq 0.25$ eV for hydrogen adatoms,[10] we obtain $R_0 \simeq 20$) and e is the effective charge of the adatom (in electron charge units), which for adsystems generally amounts to $e \simeq 0.1$–0.7.[26] Similarly, for the dipole repulsion of adatoms ($n = 3$),

$$R_0(\text{dipole}) = R_0(\text{Coulomb}) 2(z/a_s)^2 ,$$

where z is the distance between the adatom and the crystal surface. An experimental observation of the above-described devil's staircase in studying the surface diffusion on furrowed or vicinal surfaces would be a direct proof of the solitonic mechanism of diffusion in adsystems. No such results are known at present, and only observations indirectly evidencing in favor of existence of this effect can be mentioned, such as a sharp rise of D near the commensurate concentration at diffusion of adatoms on a metallic substrate[10] as well as a D increase with increasing concentration of steps on a semiconductor substrate.[54] The authors of Ref. 54 observed a jumpwise decrease of the activation energy of the surface diffusion along steps at a coverage consistent with a commensurate structure (4×2) for the Ag/Ge(111) adsystem. In a comparison with the experiment it should be taken into account that the FK model can be used to describe surface diffusion as long as the motion of atoms proceeds along one-dimensional channels. At high Θ and V_0 values, when the compression forces in the adatomic chain overcome the forces "holding" the adatoms in a given channel, adatoms will start "creeping out" of the channel so that their motion will become more complex and can be described only in terms of a two- or three-dimensional model. Moreover, it is also to be taken into account that the parameter V_0 may depend on Θ because of a mutual "depolarization" of adatoms.[23] Finally, note that the law of the interaction between adatoms in adsystems may be more complex than the power law (1.3). For example, the interaction potential for an "indirect" mechanism of interaction of adatoms has the form[23,25]

$$v(x) \sim x^{-m} \sin(2k_F x + \phi) , \tag{7.7}$$

where $m = 1$–5, ϕ is a constant phase, and k_F is the Fermi momentum for substrate electrons. In this case an attraction (or an "effective" attraction) can exist between adatoms at some distances, which in two-dimensional (as in quasi-one-dimensional) systems will result in "condensation" (first-order phase transition) of adatoms into "islands" with some concentration Θ^*.[55] The motion of kinks on the background of Θ^* should not differ qualitatively from that described above. The difference between the cases of attraction and repulsion of adatoms consists in boundary conditions: a finite-length chain with free ends (an "island" of the condensed phase) can exist in the former case, while with repulsion such a state is metastable and can exist only owing to the presence of the Peierls potential. A reflection of a kink from the chain free end is therefore possible in the case of attraction, so that the kink transforms into an antikink and moves in the reverse direction (see, e.g., Ref. 56) right up to a stop or annihilation with the next incoming kink. This effect can increase the effective diffusion coefficient in determining it, e.g., from experiments on the "creeping apart" of a step.[10]

To conclude, note that in the general case the substrate potential relief is nonsinusoidal, the parameter r of the potential (1.4) being usually negative. In this case the ε_p dependence on l is nonmonotonic and has deep local minima at some values of the parameter $l = \tilde{l}$ (see Fig. 10). Since, according to (3.11), the parameter l is proportional to coverage Θ, similar singularities of the dependence $\varepsilon_p(\Theta)$ can be expected, so that the diffusion coefficient D will have local maxima at some concentrations $\tilde{\Theta} = \Theta(\tilde{l})$.

VIII. CONCLUSIONS

Experimental studies of the surface diffusion[10] evidence an important role of a collective motion of adatoms. The Frenkel-Kontorova model is essentially a single model allowing an accurate description of such a consistent

motion of particles, which is due to the closeness of this model to the exactly integrable SG model in the continuum limit. A SG-type equation allows soliton solutions in the form of kinks. It is the small values of the effective kink mass ($m \ll m_A$) and Peierls potential ($\varepsilon_p \ll \varepsilon_A$) that cause the great contribution of kinks to diffusion and drift of adatoms.

The present study dealt with an adiabatic motion of kinks in the generalized FK model. This model is characterized by *two new aspects*: an anharmonic and a long-range character of adatom interaction. The anharmonicity of interaction results in dissimilar kink and antikink parameters, which gives rise to, e.g., a jump of diffusion characteristics when adatomic concentration Θ exceeds some Θ_0 value, corresponding to a commensurate adatomic structure. On the other hand, the long-range character of interaction between adatoms leads to an infinite sequence of commensurate structures, changing one another, with the result that dependences of the characteristics on the coverage Θ take the form of the devil's staircase.

It is clear that the proposed generalized FK model dealt with in the present study is applicable for describing not only the surface diffusion, but also quite a number of other physical phenomena, listed briefly in the Introduction; the principal restriction on the use of this model is its one-dimensional nature. Due to this, an allowance for the possibility of a motion of adatoms in a direction perpendicular to the chain appears to be a natural development of the model. Investigation of two-dimensional (both anisotropic and isotropic) adatomic structures is also of a great interest. Finally, it should be noted that in the framework of the considered extended FK model, a number of dynamical effects may be studied, in particular, to derive the equation of motion for the center of mass of a discrete kink using a recently developed projection operator approach,[57] as well as to study another nonlinear excitation, the dynamical SG soliton or breather, which may be treated in the framework of the continuum nonlocal equation. Now these problems are in consideration.

ACKNOWLEDGMENTS

The authors would like to thank Professor Yu. S. Vedula, Professor A. M. Kosevich, Professor A. G. Naumovets, and Dr. I. F. Lyuksyutov for useful discussions.

APPENDIX A: CASE OF $p=2$

Let us examine, in the continuum approximation as well, adiabatic characteristics for a more complex unit cell with $\Theta_0=2/q$, $q\equiv 2q'+1$, $q'=0,1,2,\ldots$. We introduce, according to (2.4) and (2.6), the displacements

$$\begin{aligned} x_{2j} &= -\Delta + ja + u_{1,j} \ , \\ x_{2j+1} &= \Delta + ja + u_{2,j} \ . \end{aligned} \tag{A1}$$

Minimization of the energy (2.5) leads to the equation for the vacuum displacement $\Delta=\frac{1}{2}[a_A-(-1)^{q'}\varepsilon]$,

$$\sin\Delta=\cos(\varepsilon/2)=v'(a_A+\varepsilon)-v'(a_A-\varepsilon) \ , \qquad a_A=a/2=\pi(2q'+1) \ . \tag{A2}$$

In the case of $V_0 \gg \varepsilon_A$ an approximate solution of equation (A2) has the form

$$\varepsilon \simeq \tfrac{1}{2}v''(a_A) \ . \tag{A3}$$

The further procedure of deriving a SG-type equation is as follows.[41] First, we introduce the new variables:

$$\begin{aligned} y_j &= u_{1,j} + u_{2,j} \ , \\ z_j &= u_{2,j} - u_{1,j} \ , \end{aligned} \tag{A4}$$

and then substitute (A1) and (A4) into initial equations of motion (3.4):

$$\sin(x_k)=v'(x_{k+1}-x_k)-v'(x_k-x_{k-1}) \ , \qquad k=2j,2j+1 \ , \tag{A5}$$

and linearize obtained equations in z_j. Thus, we obtain a set of equations:

$$\begin{aligned} \sin(\Delta-\tfrac{1}{2}y_j)+\tfrac{1}{2}z_j\cos(\Delta-\tfrac{1}{2}y_j) &= v'[(a_A+\varepsilon)+\tfrac{1}{2}(y_j-y_{j-1})]-v'(a_A-\varepsilon)-v''(a_A+\varepsilon)\tfrac{1}{2}(z_j+z_{j-1})-v''(a_A-\varepsilon)z_j \ , \\ \sin(\Delta+\tfrac{1}{2}y_j)+\tfrac{1}{2}z_j\cos(\Delta+\tfrac{1}{2}y_j) &= v'[(a_A+\varepsilon)+\tfrac{1}{2}(y_{j+1}-y_j)]-v'(a_A-\varepsilon)-v''(a_A+\varepsilon)\tfrac{1}{2}(z_{j+1}+z_j)-v''(a_A-\varepsilon)z_j \ . \end{aligned} \tag{A6}$$

Now we will use similarly to (4.17) and (4.18), the continuum approximation and use Eq. (4.15) for the potential $v(x)$. Taking into account that $z\sim\varepsilon$, we linearize equation (A6) in ε and neglect the terms $\sim z\varepsilon\sim\varepsilon^2$. As a result, we obtain

$$\cos(\tfrac{1}{2}y)-1-\tfrac{1}{2}(\varepsilon-z)\sin(\tfrac{1}{2}y)=-v''(a_A)(2z-\tfrac{1}{2}az')+\tfrac{1}{2}v''(a_A)(ay'-\tfrac{1}{2}a^2y'')+\tfrac{1}{8}v'''(a_A)(ay'-\tfrac{1}{2}a^2y'')^2 \ , \tag{A7a}$$

$$\cos(\tfrac{1}{2}y)-1+\tfrac{1}{2}(\varepsilon-z)\sin(\tfrac{1}{2}y)=-v''(a_A)(2z+\tfrac{1}{2}az')+\tfrac{1}{2}v''(a_A)(ay'+\tfrac{1}{2}a^2y'')+\tfrac{1}{8}v'''(a_A)(ay'+\tfrac{1}{2}a^2y'')^2 \ . \tag{A7b}$$

Adding equations (A7) together, we find the expression for the function $z(x)$:

$$z\simeq\varepsilon[1-\cos(\tfrac{1}{2}y)+\tfrac{1}{2}v''(a_A)ay'+\tfrac{1}{8}v'''(a_A)(ay')^2] \ , \tag{A8}$$

where expression (A3) for ε is used. Then we subtract equation (A7a) from equation (A7b):

$$\tfrac{1}{2}v''(a_A)a^2y''+\tfrac{1}{4}v'''(a_A)a^3y'y''=(\varepsilon-z)\sin(\tfrac{1}{2}y)+az'v''(a_A) \ . \tag{A9}$$

Substituting expression (A8) into the right-hand side of Eq. (A9), we obtain

$$\sin y-\tfrac{1}{4}v'''(a_A)(ay')^2\sin\tfrac{1}{2}y$$
$$=[v''(a_A)]^2a^2y''\left[1+\frac{v'''(a_A)}{2v''(a_A)}ay'\right]. \quad \text{(A10)}$$

Thus, equation (A10) describes a kink with the width

$$d=av''(a_A)=2ql^2/\pi . \quad \text{(A11)}$$

Using the substitution of (4.22), we transform Eq. (A10) to the canonical form:

$$\sin\bar{y}+\tfrac{1}{2}\alpha(\bar{y}')^2\sin(\tfrac{1}{2}\bar{y})=\bar{y}''(1-\alpha\bar{y}') , \quad \text{(A12)}$$

where

$$\alpha=-\frac{a_Av'''(a_A)}{dv''(a_A)}=\frac{\pi}{4}\frac{\beta_A}{l^2} ,$$
$$\beta_A=-\frac{a_sv'''(a_A)}{v''(a_A)} . \quad \text{(A13)}$$

The solution of Eq. (A12) at $\alpha\ll 1$ has the form

$$\bar{y}(\bar{x})=u_{SG}(\bar{x})+y_\alpha , \quad \text{(A14)}$$

$$y_\alpha=\frac{4\alpha}{3\cosh z}\tan^{-1}(\sinh z)-\frac{4\alpha}{3\cosh z}[1-\ln(\cosh z)] . \quad \text{(A15)}$$

The effective kink mass at $\alpha=0$ is

$$m=\sum_j[(u'_{1,j})^2+(u'_{2,j})^2]$$
$$\approx\tfrac{1}{2}\sum_j(y'_j)^2$$
$$=\frac{1}{2ad}\int d\bar{x}(\bar{y}')^2=4/(ad)=1/(ql)^2 . \quad \text{(A16)}$$

Note that the second term in the right-hand side of (A15) is even, and the first one, odd in z. This means that in calculating corrections in α to the kink characteristics in an approximation linear in α only the first term of (A15) will give a contribution. In particular, the kink mass is

$$m=\frac{4}{ad}\left[1-\frac{\alpha\sigma\pi}{6}\right]+O(\alpha^2) , \quad \text{(A17)}$$

i.e., the relative correction of the first order in the anharmonicity α is the same as at $p=1$.

Unfortunately, when interaction of only the nearest neighbors is taken into account, parameters $\varepsilon_{\text{pair}}$ and $\delta\varepsilon_p$ go to zero since they are determined by interaction between unit cells, so that their calculation needs the taking into account of interaction of atoms at distances $x\geq pa_A$. To conclude, we note that for the power-law potential (1.3) in the case of $p=2$ the kink width is

$$d=[n(n+1)V_0/\pi](2/q)^{n+1} , \quad \text{(A18a)}$$

while the anharmonicity parameter is, as before, given by the formula

$$\alpha=(n+2)/d . \quad \text{(A18b)}$$

APPENDIX B: EXPONENTIAL INTERACTION OF ATOMS

In the case of a long-range exponential interaction of atoms, (1.2), the corresponding equations of motion for the system as well, reduce in the continuum limit to a SG-type local equation (see Refs. 42 and 43). For simplicity, we will consider only kinks on the background of a coverage $\Theta_0=1$. When the interaction potential (1.2) is expanded into a Taylor series with an accuracy to cubic terms for interaction of the nearest neighbors and to quadratic terms for interaction of more remote atoms, the interaction energy of atoms will take the form

$$H_{\text{int}}=\tfrac{1}{2}\sum_{i\neq j}v(x_i-x_j)$$
$$\simeq\frac{A}{6}\sum_i(u_i-u_{i-1})^3+J\frac{1-S}{4S}\sum_{i\neq j}S^{|i-j|}(u_i-u_j)^2. \quad \text{(B1)}$$

Here we introduce the following designations:

$$S\equiv\exp(-\beta) , \quad \text{(B2)}$$

$$A\equiv-\alpha(d/2\pi)^3 , \quad \text{(B3)}$$

and

$$J\equiv(d/2\pi)^2(1-S)^{-1} , \quad \text{(B4)}$$

while parameters d and α were introduced earlier [see (4.20), (4.21), and (4.24)]. The equation of motion, which corresponds to the Hamiltonians (2.1)–(2.3) and (B1), takes the form

$$\frac{d^2}{dt^2}u_i+\sin u_i+\tfrac{1}{2}A[(u_i-u_{i-1})^2-(u_{i+1}-u_i)^2]$$
$$=J\frac{1-S}{S}\sum_{j(j\neq i)}S^{|j-i|}(u_j-u_i) , \quad \text{(B5)}$$

which can be rewritten in the form

$$\frac{d^2}{dt^2}u_i+\sin u_i+\tfrac{1}{2}A[(u_i-u_{i-1})^2-(u_{i+1}-u_i)^2]$$
$$+2Ju_i=L_i , \quad \text{(B6)}$$

where the quantity

$$L_i=J\frac{1-S}{S}\sum_{\substack{j=-\infty\\(j\neq 0)}}^{+\infty}S^{|j|}u_{i+j} . \quad \text{(B7)}$$

is introduced, which satisfies the recurrence relation[42]

$$\left[S+\frac{1}{S}\right]L_i=L_{i+1}+L_{i-1}+J\frac{1-S}{S}(u_{i+1}+u_{i-1}-2Su_i) , \quad \text{(B8)}$$

just which allows the set of Eqs. (B6) and (B8) to be reduced to a local-type equation. Going over in Eqs. (B6) and (B8) to the continuum limit and then substituting (B6) into (B8), we obtain the equation with an accuracy to terms $\sim a^3$:

$$u_{tt}+\sin u-d_{\rm eff}^2u_{xx}+\alpha d^3u_xu_{xx}=Sa^2(1-S)^{-2}f(u)\ , \tag{B9}$$

where

$$f(u)\equiv u_{ttxx}-(u_x)^2\sin u-u_{xx}(1-\cos u)\ , \tag{B10}$$

and

$$d_{\rm eff}^2\equiv d^2(1+S+S/J)/(1-S)^3\ . \tag{B11}$$

Using the substitution $x=\tilde{x}d_{\rm eff}$, we derive the equation

$$\tilde{u}_{tt}+\sin\tilde{u}-\tilde{u}_{xx}(1-\alpha_{\rm eff}\tilde{u}_x)=\varepsilon f(u)\ , \tag{B12}$$

where

$$\alpha_{\rm eff}\equiv\alpha(d/d_{\rm eff})^3 \tag{B13}$$

and

$$\varepsilon=\frac{S}{S+J(1+S)}\ . \tag{B14}$$

In the case of $d\gg a$ we have $J\gg 1$ and $\varepsilon\ll 1$; therefore, the perturbation $\varepsilon f(u)$ in Eq. (B12) in the continuum approximation can be neglected. Consequently, a long-range exponential character of atomic interaction, as compared with the above-considered short-range interactions, results only in renormalization of the kink parameters; the kink width increases ($d\to d_{\rm eff}>d$), while its nonlinearity decreases ($\alpha\to\alpha_{\rm eff}<\alpha$).

*Institute for Low Temperature Physics and Engineering, UkrSSR Academy of Sciences, 47 Lenin Avenue, Kharkov 310164, U.S.S.R.

[1]L. A. Bolshov, A. P. Napartovich, A. G. Naumovets, and A. G. Fedorus, Usp. Fiz. Nauk **122**, 125 (1977) [Sov. Phys.—Usp. **20**, 412 (1977)].

[2]A. G. Naumovets, Sov. Sci. Rev. A: Phys. **5**, 443 (1984).

[3]B. Z. Olshanetsky, V. I. Mashanov, and A. I. Nikiforov, Surf. Sci. **111**, 429 (1981).

[4]A. M. Kosevich, *Fundamentals of Crystal Lattice Mechanics* (Nauka, Moscow, 1972) (in Russian).

[5]*Solitons in Action,* edited by K. Lonngren and A. Scott (Academic, New York, 1978).

[6]F. C. Frank and J. H. van der Merwe, Proc. R. Soc. London, Ser. A **198**, 205 (1949).

[7]V. G. Bar'yakhtar, B. A. Ivanov, and A. L. Sukstanskii, Zh. Eksp. Teor. Fiz. **78**, 1509 (1980) [Sov. Phys.—JETP **51**, 757 (1980)].

[8]M. J. Rice, A. R. Bishop, J. A. Krumhansl, and S. E. Trullinger, Phys. Rev. Lett. **36**, 432 (1976).

[9]I. F. Lyuksyutov, A. G. Naumovets, and V. L. Pokrovsky, *Two-Dimensional Crystals* (Naukova Dumka, Kiev, 1988) (in Russian).

[10]A. G. Naumovets and Yu. S. Vedula, Surf. Sci. Rep. **4**, 365 (1984).

[11]S. P. Novikov, S. V. Manakov, L. P. Pitaevskii, and V. E. Zakharov, *Theory of Solitons* (Consultants Bureau, New York, 1984).

[12]A. I. Lichtenberg and M. A. Lieberman, *Regular and Stochastic Motion* (Springer-Verlag, New York, 1983).

[13]M. Peyrard and M. Remoissenet, Phys. Rev. B **26**, 2886 (1982).

[14]M. Imada, J. Phys. Soc. Jpn. **52**, 1946 (1983).

[15]Yu. S. Kivshar and B. A. Malomed, Physica **24D**, 125 (1987).

[16]S. Aubry, in *Solitons and Condensed Matter,* Vol. 8 of *Solid State Sciences,* edited by A. Bishop and T. Schneider (Springer, Berlin, 1978), p. 264.

[17]J. F. Currie, S. E. Trullinger, A. R. Bishop, and J. A. Krumhansl, Phys. Rev. B **15**, 5567 (1977).

[18]B. Joos, Solid State Commun. **42**, 709 (1982).

[19]P. Stancioff, C. Willis, M. El-Batanouny, and S. Burdik, Phys. Rev. B **33**, 1912 (1986).

[20]Y. Ischimori and T. Munakata, J. Phys. Soc. Jpn. **51**, 3367 (1982).

[21]C. Willis, M. El-Batanouny, and P. Stancioff, Phys. Rev. B **33**, 1904 (1986).

[22]Yu. S. Kivshar and B. A. Malomed, Phys. Lett. **111A**, 427 (1985).

[23]T. L. Einstein, CRC Crit. Rev. Solid State and Mater. Sci. **7**, 261 (1978); O. M. Braun and V. K. Medvedev, Usp. Fiz. Nauk **157**, 631 (1989).

[24]M. A. Vorotyntsev, A. A. Kornyshev, and A. I. Rubinshtein, Dokl. Akad. Nauk SSSR **248**, 1321 (1979); **255**, 1288 (1980).

[25]W. Kohn and K. H. Lau, Solid State Commun. **18**, 553 (1976).

[26]O. M. Braun, Fiz. Tverd. Tela (Leningrad) **23**, 2779 (1981) [Sov. Phys.—Solid State **23**, 1626 (1981)].

[27]M. Toda, *Theory of Nonlinear Lattices* (Springer, Berlin, 1981).

[28]I. Markov and A. Milchev, Thin Solid Films **126**, 83 (1985).

[29]A. Milchev, Phys. Rev. B **33**, 2062 (1986).

[30]J. C. Wang and D. F. Pickett, J. Chem. Phys. **65**, 5378 (1976).

[31]L. A. Bolshov, Acta Univ. Wratislaviensis **37**, 73 (1980).

[32]P. Bak and R. Bruinsma, Phys. Rev. Lett. **49**, 249 (1982) [see, also, survey: P. Bak, Rep. Prog. Phys. **45**, 587 (1982)].

[33]G. Wahnström, Surf. Sci. **159**, 311 (1985).

[34]*Vibration Spectroscopy of Adsorbates,* edited by R. F. Willis (Springer, Berlin, 1980).

[35]O. M. Braun and E. A. Pashitskii, Poverkhn. (USSR) **7**, 49 (1984) [Phys. Chem. Mech. Surf. **3**, 1989 (1985)].

[36]Y. Ishibashi and I. Suzuki, J. Phys. Soc. Jpn. **53**, 4250 (1984).

[37]O. M. Braun, Yu. S. Kivshar, and A. M. Kosevich, J. Phys. C **21**, 3881 (1988).

[38]I. F. Lyuksyutov and V. L. Pokrovsky, Pis'ma. Zh. Eksp. Teor. Fiz. **33**, 343 (1981) [JETP Lett. **33**, 326 (1981)].

[39]D. J. Bergmann, E. Ben-Jacob, Y. Imry, and K. Maki, Phys. Rev. A **27**, 3345 (1983).

[40]Yu. S. Kivshar, Institute for Low Temperature Physics and Engineering, Kharkov, Report No. 21/84, 1984 (in Russian); Yu. S. Kivshar and B. A. Malomed, Rev. Mod. Phys. **61**, 763 (1989).

[41]V. L. Pokrovsky and A. L. Talapov, Zh. Eksp. Teor. Fiz. **75**, 1151 (1978) [Sov. Phys.—JETP **48**, 519 (1978)].

[42]S. K. Sarker and J. A. Krumhansl, Phys. Rev. B **23**, 2374 (1981).

[43]M. Remoissenet and N. Flytzanis, J. Phys. C **18**, 1573 (1985).

[44]A. M. Kosevich and A. S. Kovalev, *Theory of Dynamic Craudions,* in *Radiation and Other Defects in Solids* (Inst. of Physics of the GSSR, Tbilisi, 1974) (in Russian); V. L. Pokrovsky and A. Virosztek, J. Phys. C **16**, 4513 (1983).

[45]Y. Hsu, Phys. Rev. D **22**, 1394 (1980).

[46]B. Joos, B. Bergersen, R. J. Gooding, and M. Plischke, Phys. Rev. B **27**, 467 (1983).

[47]R. J. Baxter, *Exactly Solved Models in Statistical Mechanics*

(Academic, London, 1982).
[48]A. Nourtier, J. Phys. (Paris) **38**, 479 (1977).
[49]A. I. Volokitin, O. M. Braun, and V. M. Yakovlev, Surf. Sci. **172**, 31 (1986).
[50]O. M. Braun and A. I. Volokitin, Fiz. Tverd. Tela (Leningrad) **28**, 1008 (1986) [Sov. Phys.—Solid State **28**, 564 (1986)].
[51]O. M. Braun, Poverkhn. **11**, 5 (1987).
[52]J. A. Combs and S. Yip, Phys. Rev. B **29**, 438 (1984).
[53]H. A. Kramers, Physica **7**, 284 (1940).
[54]E. Suliga and M. Henzler, J. Phys. C **16**, 1543 (1983).
[55]L. A. Bolshov, Fiz. Tverd. Tela (Leningrad) **13**, 1679 (1971) [Sov. Phys.—Solid State **13**, 1409 (1971)].
[56]A. S. Kovalev, Fiz. Tverd. Tela **21**, 1729 (1979) [Sov. Phys.—Solid State **21**, 813 (1979)].
[57]R. Boesch, P. Stancioff, and C. R. Willis, Phys. Rev. B **38**, 6713 (1988); R. Boesch and C. R. Willis, Phys. Rev. B **39**, 361 (1989).